C.P. No. 838

C.P. No. 838

MINISTRY OF AVIATION

AERONAUTICAL RESEARCH COUNCIL

CURRENT PAPERS

Interim Report on Low-Speed Flight Tests of a Slender-Wing Research Aircraft (Handley Page H.P. 115)

by

P. L. Bisgood and C. O. O'Leary

LONDON: HER MAJESTY'S STATIONERY OFFICE

1966

PRICE 9s 6d NET

U.D.C. No. 533.6.013.413 : 533.6.013.47 : 533.693.3 : 533.6.011.5

CP. No.838
November 1963

INTERIM REPORT ON LOW-SPEED FLIGHT TESTS OF A SLENDER-WING RESEARCH AIRCRAFT (HANDLEY-PAGE H.P.115)

by

P. L. Bisgood
and
C. O. O'Leary

SUMMARY

Tests forming part of a comprehensive programme of lateral stability measurements are described and their results discussed, together with miscellaneous supporting tests. The stability derivatives with respect to aileron deflection (ℓ_ξ, n_ξ) and sideslip (ℓ_v, n_v, y_v) have been measured by static methods, the rudder derivatives (ℓ_ζ, n_ζ, y_ζ) have been deduced from the transient response to rudder pulses, and the derivatives ℓ_v, ℓ_p, n_v, n_r, y_v and y_p have been obtained from time-vector analysis of the dutch-roll mode. Where possible, these results are compared with wind tunnel tests; the agreement is satisfactory in the case of the aileron and sideslip derivatives measured under static conditions, and ℓ_v and n_v obtained from dutch-roll analysis agree well with the 'static' results.

A brief report on the more important handling qualities is included. Contrary to expectation, the handling of the aircraft is free from serious problems.

Replaces R.A.E. Technical Note No. Aero2921 - A.R.C. 25663

CONTENTS

TABLES

ILLUSTRATIONS

1 INTRODUCTION

The 'slender wing' offers distinct performance advantages for an aircraft intended to cruise at around Mach 2, but it appeared from model and associated analytical work that such planforms might suffer from serious handling deficiencies particularly at low speeds. The Handley-Page H.P.115 slender-wing research aircraft was built to permit investigation, at low airspeeds, of the aerodynamic characteristics and the handling qualities of a configuration of this sort. The aircraft first flew on 17th August, 1961 and was handed over to the R.A.E. in November of that year. The flight testing reported here was carried out over the period December 1961-November 1962, which included about four months of non-availability.

At the time that the flight test programme was being planned, considerable concern was generally felt regarding the lateral-directional stability and control of slender wings. It was decided, therefore, to concentrate the earlier phases of the test programme on the lateral handling and the measurement of lateral stability derivatives; it was planned to make the latter measurements using a wide range of test techniques and to cover both quasi-static and dynamic conditions of flight. The data presented in the present paper include the derivatives due to aileron (ℓ_ξ, n_ξ) and sideslip (ℓ_v, n_v, y_v) measured by static methods, the rudder derivatives (ℓ_ζ, n_ζ, y_ζ) deduced from the transient response to rudder pulses, and the stability derivatives (ℓ_v, ℓ_p, n_v, n_r, y_v, y_p) obtained from analysis of the dutch-roll mode. Brief comments on the more important handling qualities are also given.

It must be emphasised that this is an interim report and that some of the quantitative information it contains may need revision in the light of further analysis, or as additional data is obtained from further tests; because of this, we have not attempted to draw any major conclusions at this stage.

2 DESCRIPTION OF AIRCRAFT

The Handley-Page H.P.115 research aircraft consists basically of a slender delta wing of 75° leading edge sweep with streamwise tips. The wing has a symmetrical bi-convex section formed by circular arcs, and its leading and trailing edges are effectively sharp (radii = 0.1 in.); the wing thickness:chord ratio is 6%.

The cockpit is somewhat underslung in order to preserve a clean dorsal line and so reduce interference over the forward portion of the wing.

The engine, a Bristol-Siddeley Viper 9 delivering a sea-level static thrust of approximately 1850 lb, is mounted above the upper surface of the rear of the wing to avoid foreign body ingestion and to ease the ground-clearance problem. The final nozzle of the jet-pipe is 'kinked' upwards by 11°, in order to minimise the pitching-moment due to thrust.

Vented, flap-type airbrakes are mounted on the lower surface of the wing and are operated pneumatically. The undercarriage is non-retracting.

A general arrangement of the aircraft is shown in Fig.1; Fig.2 shows a photograph of the aircraft in flight. The principal dimensions and leading particulars of the aircraft are given in Table 1.

All controls are manually operated. The rudder has no direct aerodynamic balance, but is fitted with a balance tab, the gearing and zero position of which can be adjusted on the ground. The full-span elevons incorporate a high degree (52%) of 'set-back hinge' balance, and two plain tabs occupy the full span of each elevon trailing edge. The outer tabs are geared in the anti-balance sense and also function as trimmers in the elevator sense; provision is made for changing the tab gearing or introducing a differential tab setting on the ground - there is no provision for lateral trimming in flight. The inner pair are spring tabs and act to reduce the stick forces once a small preload has been exceeded. A 'feel spring' is incorporated in the elevator circuit, near the base of the stick, and is disengaged when the trimmer is operated. This rather complicated control system provides reasonable and well-harmonised aileron and elevator forces, though the system has some disadvantages from the flight-test point of view.

The aircraft structure is fabricated from light alloy components and covered with light alloy sheeting; the exceptions to this are (a) the main control surfaces, which, broadly speaking, are ply-covered ahead of the hinge line and fabric-covered aft, and (b) the detachable leading edge, which has a plywood covering over spruce frames. Strong points are provided near the extremities of the fuselage and the wing tips, which can be used to mount ballast and so change the c.g. position and the moments of inertia.

3 DESCRIPTION OF INSTRUMENTATION

The flight parameters measured are listed in Table 2, together with the transducers used and their characteristics; these parameters were recorded in two continuous-trace galvanometer recorders*, fed by a common time-base. The pilot noted the fuel state and engine conditions appropriate to each run, obtaining the former from an accurate fuel flowmeter which incorporated a 'gallons remaining' counter.

The dynamic characteristics of the rate gyroscopes were quite acceptable, though the traces they produced contained small amounts of high-frequency noise which originated in the rotor and gimbal bearings and tended to increase as these bearings wore. Angular acceleration information in roll and yaw was obtained, in effect, by measuring the damping currents generated by motion of the gimbal systems of the rate gyroscopes; since the 'noise' referred to above was differentiated (and hence amplified) by this process, the noise content of the acceleration traces was relatively high, even with rather heavy filtering. The rate gyroscopes were rigidly mounted in the aircraft and their measurement axes were aligned within 0.04° of the relevant body datum axes.

The accelerometers had adequate dynamic characteristics, and although they suffered from slight cross-sensitivity, this had no significant effect on the results reported here, which relate to a substantially uniform 1g field. They were mounted as close as practicable to the aircraft's c.g. It should be noted that though the lateral accelerometer was the best available at the time, it was less sensitive than was desirable.

* The choice of recorders was compromised to some extent by the limited weight and space available.

Control and tab angles were measured by miniature, commercially-available A.C. transducers; it was found that the transducers used initially to measure elevon angles had undesirable dynamic characteristics and they were replaced by R.A.E. designed equipment of adequate performance.

Pitch attitude relative to the resultant acceleration vector in the plane of symmetry was measured by a pendulum inclinometer.

A fairly short and stiff boom, mounted in the plane of symmetry and parallel to the chord-line, extended forward from the lower surface of the fuselage nose (Fig.1). At its forward end this boom carried a standard Mk.9 pitot-static head which supplied total pressure to the A.S.I. system, and static pressure to the altimeters and the pilot's A.S.I. A small venturi was fitted on the starboard side of the boom and connected to the 'static' side of the airspeed recording element, thus effectively amplifying the airspeed signal to a level consistent with the recording instrument's sensitivity. Incidence and sideslip vanes were mounted, respectively, on the port and lower surfaces of the boom and drove potentiometer pick-offs.

The equipment for measuring elevator and aileron stick forces was used only during the early stages of the development flying.

4 FLIGHT TEST METHODS

4.1 Range of tests

For the majority of the tests described below, the aircraft's all-up weight at engine starting was approximately 5050 lb with the maximum fuel load of 1170 lb. The centre of gravity was at 54.8% of the centre line chord (c_o) with full fuel load, and moved forward to 54.7% as the tanks emptied. Exceptions to these conditions are noted where appropriate.

Because there was little interest in the aircraft's 'high speed' behaviour the tests were limited to the maximum speed attainable in level flight (about 175 knots I.A.S., depending on weight and height). The lower limit of airspeed was reduced progressively during the programme, the lowest speed reached being 50 knots, while the lowest speed at which tests have been made regularly is 60 knots. The angles of incidence corresponding to this range of test airspeeds (175-60 knots) ranged from 4^{o} to 24^{o}, approximately.

The majority of the tests were made at a height of 10,000 ft.

4.2 Position error measurements

Because the airspeed and incidence sensing elements were subject to influence by the aircraft's pressure field, it was considered essential to calibrate them in flight. Two techniques were used:-

(a) The 'aneroid' method. The aircraft was flown past an observing station on the roof of a high building at various stabilised airspeeds; the readings of sensitive aneroids, at the observing station, and in the aircraft and connected to its static pressure source, were compared to yield static

position error. The method became increasingly prone to error as the dynamic pressure decreased, and the majority of the low-speed P.E's were obtained by

(b) The 'formation' method. A slight modification of this standard technique was employed in that the tests were made above fairly strong low-level (2000-4000 ft) inversions; this ensured suitably smooth conditions and also provided a well-defined 'top' to the haze layer and hence an excellent horizon against which the test aircraft could be photographed for attitude measurement and height correction. An example of such a photograph is shown in Fig.2.

Some further checks on the incidence vane calibration were obtained from measurements of attitude and flight path inclination taken under steady flight conditions (e.g. during partial glide tests).

4.3 Partial glides

To maintain level flight, the H.P.115 requires a thrust which is a relatively large fraction of its weight; furthermore, the angle between the thrust vector and the flight path may be large, particularly at low speeds; in consequence the thrust component normal to the flight path can be significant (about 10% of the weight in an extreme case), and must be allowed for when computing lift coefficients, for example. These corrections were derived from approximate measurements of the aircraft's performance obtained by partial glide tests.

The aircraft was established in a steady glide (engine idling) at the desired airspeed and at an altitude of about 12,000 ft. Records were taken as the aircraft passed through 10,000 ft altitude and, in addition, the pilot measured with a stop-watch the time taken to descend through a given height band (usually from 11,000 to 9000 ft). The tests were repeated at various speeds distributed throughout the normal speed range.

4.4 Lateral and directional stability tests

4.4.1 Steady sideslips

Starting from trimmed, level flight at 10,000 ft, the pilot made a series of straight steady sideslips in each direction, up to maximum angles of $\pm 5^{\circ}$, maintaining constant height and airspeed; records were taken only when each particular condition had been stabilised. The tests were repeated at various speeds distributed throughout the level flight range.

The above procedure was repeated with ballast weights mounted in one of the wing-tips (together with sufficient ballast in the nose to maintain the longitudinal c.g. position at 0.548 c_o), all weights being mounted internally. Initially, a few handling checks were made with 50 lb mounted in the starboard wing-tip. The ballast was then increased to 95 lb (the maximum available) and steady sideslip measurements made throughout the speed range. These tests were repeated with 95 lb of ballast in the port wing-tip. The all-up weight at take-off was approximately 5190 lb when carrying 95 lb of wing-tip ballast.

In all the above tests, the records showed slight control buffeting at moderate sideslip angles, and this increased in intensity with increasing

sideslip and incidence. The buffet was often confined to, and was always more severe on, the leading elevon. However, this did not constitute a handling problem but probably reduced slightly the accuracy with which elevon angles could be measured at the larger angles of sideslip.

4.4.2 Lateral oscillations

The aircraft was trimmed for straight and level flight at 10,000 ft. The recorders were then switched on and a rapid 'pulse' of rudder injected by the pilot. After returning the rudder to its trimmed position (approximately), and throughout the ensuing dutch-roll oscillation, the pilot attempted to hold all controls fixed. As an alternative technique, some oscillations were initiated by a double pulse of aileron, the controls again being held fixed during the subsequent motion. Recording was continued until the oscillation had decayed to small amplitude or a sufficient number of cycles had been recorded; in the case of divergent oscillations, the bank amplitude was allowed to increase to about 10° and the pilots then resumed control.

In general the pilots were only partially successful in their efforts to hold the controls fixed, at least while the oscillation amplitude was fairly large - in the case of the elevons this was due, in part, to the absence of a rigid connection between stick and control surface, which is inherent in a spring-tab control system.

It should be noted that the thrust available at 10,000 ft was not sufficient to maintain level flight at the lower test airspeeds (below about 70 knots, depending on weight), and data were obtained during slow descents at full throttle. A limited amount of supplementary low-speed data was obtained in level flight at reduced test altitude (5000 ft).

To investigate the possible influence of engine conditions on the aerodynamic derivatives, a number of lateral oscillations were recorded on the glide (i.e. engine idling) at 10,000 ft.

5 METHODS OF ANALYSIS

5.1 Steady sideslips

The control angles and lateral accelerations measured during these tests were plotted against indicated sideslip, and the values of these quantities at zero indicated sideslip were read off the resulting curves for each test airspeed, plotted against C_{La} for the two (95 lb) asymmetric ballast conditions, and faired curves drawn. The changes ($\Delta\xi_o$, $\Delta\zeta_o$ and Δa_{y_o}) between the two ballast conditions at given values of C_{La} were read off these curves; these changes were related to the control derivatives and to the change, ΔL, in applied rolling moment by the expressions,

$$\left.\begin{aligned} \ell_\xi \Delta\xi_o + \ell_\zeta \Delta\zeta_o &= \frac{\Delta L}{\frac{1}{2}\rho V^2 Sb} = C_{La} \frac{\Delta L}{Wb} \\ n_\xi \Delta\xi_o + n_\zeta \Delta\zeta_o &= 0 \\ y_\xi \Delta\xi_o + y_\zeta \Delta\zeta_o &= \frac{m \Delta a_{y_o}}{\rho V^2 S} = \frac{C_{La}}{2} \frac{\Delta a_{y_o}}{g} \end{aligned}\right\} \quad (1)$$

It was possible, therefore, to determine the aileron derivatives from these expressions by substituting therein values for the rudder derivatives obtained from flight or wind-tunnel tests.

For the case of steady, straight flight, the equations of motion can be differentiated with respect to sideslip to give

$$\left.\begin{aligned} \ell_v + \ell_\xi \frac{d\xi}{d\beta} + \ell_\zeta \frac{d\zeta}{d\beta} &= 0 \\ n_v + n_\xi \frac{d\xi}{d\beta} + n_\zeta \frac{d\zeta}{d\beta} &= 0 \\ y_v + y_\xi \frac{d\xi}{d\beta} + y_\zeta \frac{d\zeta}{d\beta} - \frac{C_{La}}{2} \frac{d\, a_y}{d\beta} &= 0 \end{aligned}\right\} \quad (2)$$

The plots of ξ, ζ and a_y against indicated sideslip were essentially linear for moderate angles and the slopes of these linear portions were measured, plotted against C_{La}, and faired curves drawn. The position error of the sideslip vane has yet to be determined experimentally and so the correction from indicated to true sideslip was estimated[2,3] and applied to the faired values making allowance for the fact that the vane senses $\tan^{-1} \frac{v}{U \cos \alpha}$. These data were used, in conjunction with the control derivatives, to determine the sideslip derivatives from equation (2).

5.2 Lateral oscillations

The analysis of the dutch-roll records has been divided into two parts, the first of which deals with the transient response to the control pulse while the second deals with the lateral oscillation proper.

5.2.1 Transient response

The immediate response of an aircraft to an abrupt control pulse of short duration is dominated by the inertial characteristics, the aerodynamic forces and moments (other than those generated by the control) being small at that stage. Thus, to a first approximation, the initial response to rudder can be written

$$\left.\begin{aligned} L_\zeta \Delta_\zeta &\doteq A \Delta\dot{p} - E \Delta\dot{r} \\ N_\zeta \Delta_\zeta &\doteq C \Delta\dot{r} - E \Delta\dot{p} \\ Y_\zeta \Delta_\zeta &\doteq m \Delta a_y \end{aligned}\right\} \qquad (3)$$

where Δ here denotes the increment from the original steady condition.

Records for analysis were selected on the criteria of steadiness prior to the pulse and brevity of pulse duration. The peak control displacements during the pulses and the peak linear and angular accelerations resulting therefrom were measured from the flight records and corrected, approximately, for the frequency response of the instruments; the lateral accelerometer readings were then corrected for the offset of the instrument from the aircraft's c.g. The first approximations to the control derivatives were then calculated from equation (3), using the measured aircraft weights and the moments and products of inertia* appropriate to those weights.

The aircraft response parameters p, r and β at the instant of peak control displacement, were obtained from the flight records, and the associated aerodynamic forces and moments were calculated using wind-tunnel data or estimates of the derivatives; these were then used to correct the approximate control derivatives.

Up to this point it was convenient to work in body axes, since the majority of the essential parameters were measured in that system. The body-axis control derivatives were converted to the stability axis system, using the measured incidence, by the relationships

$$\ell_\zeta = \ell_{\zeta B} \cos\alpha + n_{\zeta B} \sin\alpha$$

$$n_\zeta = n_{\zeta B} \cos\alpha - \ell_{\zeta B} \sin\alpha$$

$$y_\zeta = y_{\zeta B}$$

It was observed that a rudder pulse was frequently accompanied by a small, inadvertent, movement of the ailerons and corrections for this were applied, where necessary, after the conversion to stability axes.

5.2.2 Dutch-roll analysis

In this preliminary analysis, the usual assumptions of lateral stability theory have been made; in particular it was assumed,

---

* Recent measurements have shown the actual inertia to differ significantly from the estimates (see Table 1). The results reported in the present paper are based on these measured inertias. The inertia measurements will form the subject of a separate note.

(a) that the aircraft behaved as a linear system, the disturbances were small, and their squares and products negligible,

(b) that there was no coupling between the lateral and longitudinal modes.

The first assumption may not be strictly valid for this aircraft, but we do not have the means to undertake rigorous analysis of a non-linear system at the present time. Some longitudinal-lateral coupling was recorded, but this was invariably small and its effects have been neglected in the present analysis.

The dutch-roll components of the total response were analysed by time-vector methods. The principles of the 'time-vector' method are well-established and a good description of their practical application is given in Ref.5; a resumé of the methods employed here (which are essentially similar to those of Ref.5) is given below.

The flight records included the initial control transient, followed by a relatively short interval during which the response contained a significant contribution from the roll subsidence; these portions were excluded from the dutch-roll analysis. The few flight records which contained relatively large contributions from the spiral mode (due, usually, to a failure to return the rudder to its trimmed position) were also discarded; the spiral mode component was filtered out of the remaining records by establishing graphically for each variable the true datum about which the oscillation occurred.

For each oscillation analysed, successive peak amplitudes from the true datum were plotted on a logarithmic scale against number of cycles for each of the recorded variables, and the best set of parallel straight lines drawn. The damping was determined from the slope of these lines, and the ratio of the ordinates of any pair of lines at a particular abscissa defined the amplitude ratio of the quantities represented.

The instants at which the oscillating quantities intersected the appropriate datum lines could be determined with reasonable accuracy; these were plotted against number of cycles for each variable, and the best set of parallel straight lines drawn. The frequency of the oscillation and the apparent phase angles between the variables were determined from these plots, and the latter were then corrected for instrument phase lags to give true phase angles.

For analysis in stability axes the roll and yaw rate data were transformed from body (datum) axes, using the time-vector relationships

$$\bar{p} = \bar{p}_B \cos \alpha + \bar{r}_B \sin \alpha$$

$$\bar{r} = \bar{r}_B \cos \alpha - \bar{p}_B \sin \alpha$$

The noise content of the angular acceleration signals made it difficult to measure their amplitudes or phases with sufficient precision for analysis, and

it was considered preferable, therefore, to derive this information from the angular velocity data by means of the well-known relationships between time-vectors and their derivatives.

The lateral acceleration at the c.g. was derived from the accelerometer reading by the vector relationship*

$$\bar{a}_y = \bar{a}_{y_i} - x_1 \dot{\bar{r}}_B + z_1 \dot{\bar{p}}_B$$

where (x_1, y_1, z_1) denote the coordinates of the accelerometer relative to the c.g.

Because some doubt was felt regarding the accuracy of the sideslip vane under dynamic conditions, the angle of sideslip was derived from the kinematic relationship

$$\frac{\bar{a}_y}{g} = \frac{V}{g}(\bar{r} + \dot{\bar{\beta}}) - \bar{\phi}\cos\gamma - \bar{\psi}\sin\gamma$$

where γ is the inclination of the flight path to the horizontal, and

$$\phi = \int p.dt \; ; \quad \psi = \int r.dt \; .$$

Some of the records analysed showed appreciable oscillation of the controls, usually the ailerons. The amplitudes and phase angles of these control movements were obtained by methods similar to those employed for the other flight parameters, but in general the amplitudes were small and, consequently, the phase information was rather inaccurate.

From the amplitude and phase relationships established between the flight variables, it was possible to solve the equations of motion by time-vector methods, assuming values for one aerodynamic derivative in each of the three equations; estimated values of the derivatives ℓ_r, n_p and y_r were employed, and the inertia data were obtained experimentally.

6 RESULTS AND DISCUSSION

6.1 Position error measurements

The flight test data were reduced by standard methods to yield total position error. The 'datum height' method yielded only static P.E., and in

---

* The small term $y_1 (p_B^2 + r_B^2)$ has been omitted from the R.H.S., in conformity with the basic assumptions; its effect could be regarded approximately as the addition of a 2% second harmonic component to the $\dot{p}_B$ term, distorting the wave form without changing either amplitude or mean phase.

this case the pitot P.E. was obtained from wind-tunnel measurements[1]. The total position-error corrections are plotted against I.A.S. in Fig.3; these corrections were used to calibrate the airspeed recorder in terms of E.A.S.

It will be seen from Fig.3 that the P.E.C. shows considerable scatter (about ±1.2 knots, max) at the lower airspeeds, due to the difficulties of accurate measurement at low dynamic pressures. It is probable that the P.E.C. curve is accurate to about ±0.5 knots down to the lowest speed for which it could be established (about 70 knots); the extrapolation to lower airspeeds may increase the possible inaccuracy. Due to the possible errors in P.E.C., the aerodynamic coefficients and derivatives obtained may be in error by up to ±1.5% at speeds above 70 knots, and perhaps ±3% at the lowest normal test airspeed (60 knots).

The data obtained during flight calibration of the incidence vane are presented in Fig.4, which also includes supplementary data obtained in other well-stabilised flight conditions. It will be seen that the mean scatter is reasonably low (about $\pm\frac{1}{4}^{\circ}$).

It may be noted that the slight 'hump' in the incidence curve corresponds closely with the region of near-constant P.E. (85-110 knots, Fig.3), suggesting that both features may have a common origin.

6.2 Partial glides

Lift-drag ratios were derived from the partial glide test data, using values for the nett idling thrust estimated from the engine brochure, and the results are shown plotted against lift-coefficient in Fig.5.

These results were found to agree reasonably well with comparable wind-tunnel data*, being about 5% higher than the latter throughout the test range. This difference is attributable in part to the higher Reynolds number of the flight tests.

The lift-drag ratios of Fig.5 were used to correct the flight results from apparent to true lift coefficient, where, for level unaccelerated flight

$$C_{La} = C_L \left(1 + \frac{D}{L_1} \tan \alpha_T\right) = \frac{W}{\frac{1}{2}\rho V^2 S}$$

α_T being the thrust-line incidence. This expression is not strictly correct since the lift-drag ratio is influenced by elevator angle to trim. It will be seen from Fig.6, however, that the effects of power on elevator angle to trim were small, so that the errors introduced by this simplifying assumption were small also.

---

* The wind-tunnel data referred to here and elsewhere in this section were obtained from tests made on a $\frac{1}{8}$th scale model in the 13' x 9' tunnel at R.A.E. Bedford. It must be emphasised that these data should be regarded as provisional at the present time.

In Fig.7 the apparent and true lift coefficients for a number of level flight runs have been compared. The tunnel C_L - α curve relevant to flight elevator angles to trim has been included in the figure and is in excellent agreement with the flight data for incidences below 17°; at 20° incidence, however, the flight C_L is higher by about 3%, which may be due to errors in P.E.C. at these low speeds (para.6.1).

6.3 Steady sideslips

A typical plot of control angles and lateral acceleration against indicated sideslip is shown in Fig.8. It will be seen that the aileron and rudder angles varied linearly with sideslip over the test range and that the range of linearity of lateral acceleration was somewhat smaller. Elevator angle to trim was only slightly affected by sideslip, indicating that m_v was small.

The control angles to trim at zero indicated sideslip are plotted against C_{La} in Fig.9 for the two 95 lb asymmetric ballast conditions. It was observed that these angles changed rather abruptly (as indicated by the dashed lines in Fig.9) over a small C_L range centered around $C_{La} \doteq 0.52$; this appears to have been caused by a sudden change in local flow direction near the vane rather than a genuine change of directional trim, but the causes of the phenomenon have yet to be established. Except in the region where the apparent vane zero-shift occurred, the mean curves of aileron angle to trim were reasonably well established and the scatter of individual points was small. However, rudder angles to trim were less satisfactory in this respect.

The lateral accelerations at zero indicated sideslip were always small so that the scatter of results tended to be relatively large; furthermore, several runs had to be discarded owing to sticking of the accelerometer.

The aileron derivatives (ℓ_ξ, n_ξ) were calculated by the method outlined in para.5.1, using values of ℓ_ζ and n_ζ obtained from flight (see para.6.4) and from wind-tunnel tests, and the results are shown in Fig.10. Both flight and tunnel values of ℓ_ζ were small compared with ℓ_ξ, so that the latter was not sensitive to possible errors in the incremental rudder angles ($\Delta\zeta_o$) but depended primarily on the accuracy with which the incremental aileron angles ($\Delta\xi_o$) could be determined; this is believed to be in the region of ±0.1°, so that ℓ_ξ should be accurate to about ±10% in the worst case (at high speed, where $\Delta\xi_o$ is about 1°); the values of ℓ_ξ based on the individual data points of Fig.9 (rather than on the mean curves) have been included in Fig.10 and show a mean scatter of ±3%. The flight values of ℓ_ξ agree well with the tunnel at the lower speeds, but become numerically lower by about 10% at the highest speeds tested; the latter could well be a genuine aero-elastic effect. We have noted already that the quality of the flight-measured rudder angles to trim was not entirely satisfactory, so that the values of $\Delta\zeta_o$ could not be defined within

close limits; in consequence, the values of n_ξ derived therefrom were felt to be in some doubt. In these circumstances it was not surprising to find rather poor agreement (±25%) between flight and tunnel values of n_ξ, though it should be noted that part of this discrepancy may be attributable to the effects of scale on the flow through the control hinge gaps.

Because of the difficulty experienced in measuring lateral acceleration to a sufficient order of accuracy, only tentative values of y_ξ could be extracted from the flight data; these values were broadly similar in magnitude to the tunnel results, ranging from about 0.03 to 0.06. This uncertainty has led us to use wind-tunnel data for y_ξ in the computation of y_v from equation (2).

The rates of change of the control angles and the lateral acceleration with indicated sideslip angle are shown in Fig.11 as functions of C_{La}. The sideslip derivatives were calculated from these data, as outlined in para.5.1, using the flight-measured control derivatives (except in the case of y_ξ), and the results are shown in Fig.12, together with the estimated correction to indicated sideslip used in the calculation. Because we had some reservations regarding the accuracy of the flight-measured control derivatives (other than ℓ_ξ), the calculations were repeated using wind-tunnel values for all the control derivatives, and the results have been included in Fig.12. The differences between the values of ℓ_v obtained by these two processes are small, and both sets of results agree well with the provisional wind-tunnel results.

The values obtained for n_v by substituting flight-measured values of the control derivatives in equation (2) are in excellent agreement with the provisional wind-tunnel results (see Fig.12); this must be considered fortuitous, to some extent, in view of the uncertainties involved in the extraction of n_ξ from the flight data. The agreement became poor when wind-tunnel values of the control derivatives were used in the substitution; this effect arose mainly from the differences between flight and wind-tunnel values of n_ζ (see para.6.4). It should be noted here that the wind-tunnel $C_n - \beta$ curves were slightly non-linear (a feature not reflected by the control angles to trim in flight) and the tunnel results referred to above relate to a range ($0-5^\circ$ of sideslip) corresponding to that used in flight (about $\pm 4^\circ$, usually).

Values of y_v extracted from the flight data are in reasonable agreement with the provisional wind-tunnel results.

6.4 Rudder derivatives from transient response

The initial transients in the response to rudder pulses were analysed by the method outlined in para.5.2.1 to yield the rudder derivatives ℓ_ζ, n_ζ and y_ζ. The corrections for changes in p, r and β were small in the case of $n_{\zeta B}$ and $y_{\zeta B}$ so that these results are insensitive to errors in the corrections themselves

(e.g. due to errors in estimating the derivatives involved). In the case of $\ell_{\zeta B}$, however, the corrections were larger - up to 20% of the total value. It should be noted that in the transformation to stability axes ℓ_ζ occurred as the small difference between comparable quantities; this, coupled with the relatively large corrections necessitated by the small, inadvertent, aileron movements (para.5.2.1), made for poor accuracy in ℓ_ζ.

The results of this analysis are shown in Fig.13, plotted against C_L. The rather large scatter is attributable mainly to the high noise content of the angular acceleration traces (see para.3) and, in the case of y_ζ, to the very small accelerations measured. Although these results show broadly similar trends to the provisional wind-tunnel results, the flight values for n_ζ and y_ζ are numerically larger by up to 25%; it seems most unlikely that these discrepancies could be attributed wholly to scale effect, nor does it appear that the instrumentation could have been in error to this extent, though this possibility will be investigated further. Measurement of the rudder derivatives by 'static' methods is planned for the future, and may help to resolve this problem. In view of the potential inaccuracies inherent in extracting ℓ_ζ from the flight data, the results are considered to agree well with the wind-tunnel.

6.5 Dutch-roll results

The variation of the dutch-roll period, damping and roll/yaw ratio (in stability axes) with C_L are shown in Fig.14. The bulk of this data relates to level flight at 10,000 ft or, at the higher C_L's (>0.55 approximately) where there was insufficient thrust for level flight, to slow descents at maximum continuous power. The few results obtained with engine idling at 10,000 ft or in level flight at 5000 ft did not differ significantly from the main body of the data.

Vector polygons typical of the various preliminary stages in the analysis are shown in Fig.15, and in Fig.16 the method of solving the equations of motion by closure of the appropriate vector polygons is evident; the values assumed for the derivatives ℓ_r and n_p which were used in these solutions are shown in Fig.17 - the derivative y_r was assumed to be zero.

It should be noted that in deriving the c.g. lateral acceleration we have neglected the variation in c.g. height with fuel state (i.e. in z_1 in Fig.15(a)). This omission introduced small errors in the amplitude and phase of a_y, the main effects of which were, firstly, to introduce a bias in the mean values for y_p and y_v, making their apparent values less positive by about 0.02 for y_p and about 5% or less for y_v, and, secondly, to increase the scatter in y_p (and to a lesser degree in y_v).

The derivatives obtained by vector analysis of the dutch-roll data did not differ significantly between the three flight conditions covered in the tests, and they have been plotted against lift coefficient in Figs.18, 19 and 20.

The results obtained for ℓ_v (Fig.18) show relatively little scatter and agree reasonably well with those obtained from steady sideslip tests and from the wind-tunnel. The data show a slight, but perhaps significant, tendency for the 'dynamic' ℓ_v to become numerically less than the static value as the reduced frequency parameter, $\nu \left(= \frac{\omega s}{V}\right)$, increased (i.e. in this case, as C_L increased); this trend, if substantiated by an extension of the present tests, is qualitatively similar to that found by Owen in some wind-tunnel experiments on a gothic wing (unpublished).

The damping in roll, ℓ_p, agrees well with the estimated values at lift coefficients below about 0.4, but becomes numerically less than estimated at higher C_L's (Fig.18). The results are somewhat scattered and the reasons for this (which apply with even greater force to the scatter observed in n_r and y_p) become clear on examining the vector diagrams of Fig.16, where the sensitivity of these derivatives to possible errors in phase measurement is immediately obvious; the relative phases between the various flight parameters cannot be established to an accuracy much better than $\pm 2^\circ$ with the existing instrumentation, and in practice the phase errors may be slightly larger than this and could account for much of the scatter observed.

The results obtained for n_v (Fig.19) agree reasonably well with those derived from steady sideslip tests (based on the flight-measured control derivatives). The sideslip amplitude in the dutch-roll tests was generally less than $\pm 2^\circ$, whereas the range covered in the steady-sideslip tests was usually about $\pm 4^\circ$. Assuming that there is no difference between steady and oscillatory values of n_v in this case, the agreement between the two sources would indicate that, within the experimental accuracy, the n_v measured in flight was independent of sideslip amplitude over the range quoted; this is in contrast with the wind-tunnel results, which exhibited the slight non-linearities in the $C_n - \beta$ curves, usual for this type of configuration*.

The results for n_r show a marked scatter, the main causes of which have been mentioned above. It should be noted that the values obtained for n_r in this analysis were influenced strongly by the values assumed for n_p, particularly at low C_L; because of this, the rapid increase in n_r at low C_L's, shown in Fig.19, may not be genuine. Tests aimed at measuring n_r by other methods are currently in progress, and it is hoped that these will resolve some of the present

---

* The wind-tunnel values given in Fig.12 are for a $\pm 5^\circ$ range of sideslip, to give the nearest available comparison. For the range $\pm 2^\circ$, n_v was about 80% of these values.

uncertainties; subsequent re-analysis of the dutch-roll data in the light of this information may enable us to establish values for n_p.

The analysis yielded rather unsatisfactory results for the side-force derivatives (Fig.20). The values obtained for y_v are extremely scattered and the mean curve differs from the steady-sideslip results by up to 25%; it is thought that this may have been due to the very small lateral accelerations involved (with very few exceptions these were less than 0.02g) for which the available instrumentation proved insufficiently sensitive or accurate.

The scatter of the results for y_p is thought to have arisen partly from insensitivity of the lateral accelerometer, and partly from the sensitivity of y_p to random errors in phase measurement; the discrepancy between measured and estimated values of y_p (Fig.20) could be explained by a consistent error of about 2° in the phase of a_y. It should be noted here that consistent errors in the magnitude and phase of a_y, sufficient to account for the observed discrepancies in y_v and y_p, would have little influence on the rolling and yawing moment derivatives obtained by this analysis.

7 HANDLING*

The handling qualities predicted for the H.P.115 during the design stage were far from encouraging, based on existing criteria; two features which gave particular cause for concern were:-

(a) the dutch-roll characteristics, which seemed likely to constitute a serious handling problem, especially at the lower flight speeds, and

(b) the difficulties likely to be encountered in making a cross-wind approach and landing, especially in turbulent conditions, seemed likely to restrict drastically the conditions in which the aircraft could be flown.

In practice, the lateral handling behaviour has proved to be remarkably docile, despite the fact that the actual dutch-roll behaviour does not differ greatly from that predicted. The measured dutch-roll characteristics are compared with the handling criterion** of Ref.6 in Fig.21, and, on the basis of this

---

* In this section, direct quotations from pilot's reports appear between inverted commas.

** This criterion was established by extensive flight tests under simulated approach conditions during which the dutch-roll period was substantially constant at 3.5 secs and the aileron yawing moment (n_ξ) was maintained at 'optimum' levels. It related pilot opinion to the damping of the oscillation (in terms of $1/T_{\frac{1}{2}}$) and the parameter $\left|\frac{\phi}{v_E}\right|$ (where $\left|\frac{\phi}{v_E}\right| \div \frac{57.3}{V\sqrt{\sigma}} \left|\frac{\phi}{\beta}\right|$ is the amplitude ratio of bank to equivalent side-velocity). It is thought that the difference in period from that of the H.P.115 should not influence the applicability of this criterion significantly.

criterion, it is evident that the H.P.115 dutch-roll would be rated as 'acceptable for normal operation' only at speeds greater than about 130 knots ($C_L \leq 0.15$), and would be rated 'unacceptable' for speeds less than about 95 knots ($C_L \geq 0.3$); in practice, the actual ratings assigned by the pilots were considerably better than these - for example, at 60 knots ($C_L \div 0.65$) the aircraft was rated 'acceptable' (rating $\div$ 4) in calm air and 'marginally acceptable' (rating $\div$ 6.5) in mild turbulence, while at 95 knots the ratings improved to 'satisfactory' (ratings of 2.5-3) in calm air and 'acceptable' (ratings of 3.5-4.5) in moderate turbulence; the fact that 95 knots is a commonly used touch-down speed, and has been used as an approach speed, lends added weight to these latter ratings. Though the reasons for these unexpectedly favourable opinions are not fully understood, the pilots' comments indicate a keen awareness of the high rolling acceleration of this aircraft (it has been referred to as "a bundle of rolling accelerations") and suggest that the instinctive reaction to these accelerations, in conjunction with the high quality of the roll control, is sufficient to check a disturbance "before a significant displacement has occurred". The remarkable precision of control achievable has been demonstrated by allowing the dutch-roll to diverge at low airspeeds, with controls fixed; the oscillation stabilised eventually at bank amplitudes in the region of $\pm 30^{\circ}$, the pilot then "comfortably and instinctively corrected with aileron movements" and, in about 5 seconds, had restored the aircraft to substantially steady, wings-level flight at the same airspeed; conversely, "normal, instinctive lateral control movements" have been used to prevent development of the dutch-roll divergence at low airspeeds. In this connection, it should be mentioned that the lateral control has been described as "rather like flying an aircraft with pleasantly powerful and sensitive powered ailerons"; the response is "crisp and rapid", and the control movements required are small and transient with "an associated pleasantly resilient feeling - the result is that the forces seem much lower than they are in reality"; only when prolonged aileron deflections are needed (e.g. in a steady sideslip) does the pilot appreciate the relatively high forces required.

The approach and landing in cross-winds has proved to be far less difficult than had been feared during the design stage, the maximum cross-wind component in which the aircraft has been operated to date being about 18 knots in a total wind strength of about 22 knots (accompanied, of course, by the low altitude turbulence typical of such a wind), when the approach and landing was described as "moderately hard work, but not particularly difficult". Many flights have been made in cross-winds of the order of 15 knots and both 'crabbing and 'sideslipping' techniques have been used on the approach, without difficulty. It is reasonable to infer from this result that a similar but larger aircraft (e.g. comparable to some S.S.T. proposals) would be capable of making a successful approach in cross-winds equivalent to these angles of sideslip (i.e. about 10°, or roughly 25 knots cross-wind at an approach speed of 150 knots), but it does not follow that the terminal manoeuvre (removal of drift or sideslip) would necessarily be as simple in the larger aircraft since the problems of height judgement, timing, etc, may be quite different and the aircraft geometry may impose more stringent limits on permissible touch-down attitudes. In the latter connection it should be noted that the H.P.115 has a relatively generous tip clearance in the landing attitude (equivalent to about 10° of bank with compressed oleos, tail bumper on the ground, and control neutral), so that the pilots may have tended to be more

tolerant of bank errors in the final stages of the approach than they might otherwise have been. Exceptionally, bank errors of up to 5° at touch-down have been noted, following a sudden cross-wind gust.

The ground behaviour during cross-wind take-offs or landings is of some interest. During the take-off run the aircraft tends first to weathercock into wind then, as airspeed increases, it rolls out of wind and shortly afterwards tends to yaw out of wind; finally, at still higher airspeed, the normal weathercock tendency reappears. The behaviour during the landing run is similar, but the sequence of events is, of course, reversed. These characteristics are common, in varying degrees, to other aircraft of rather 'slender' configurations and it is thought that the out-of-wind yaw results from differential undercarriage loads associated with the 'out-of-wind' rolling moment.

The majority of the approaches to date have been made at speeds in the 110-120 knot band, using about one-half airbrake extension; however, a number of approaches have been made, without difficulty, in the 'clean' condition at speeds down to 95 knots* - in this condition the aircraft is well below the minimum drag speed, and though it just satisfies the criterion for 'minimum comfortable' speed for carrier approaches, put forward in Ref.7, namely

$$-\frac{C_L}{W/S}\left(\frac{C_D}{C_L}-\frac{dC_D}{dC_L}\right) \geq 0.003$$

it does not meet the criterion for a standard airfield approach[7]

$$-\frac{C_L}{W/S}\left(\frac{C_D}{C_L}-\frac{dC_D}{dC_L}\right) \geq 0.001 \ .$$

At these speeds the aircraft was rated as 'satisfactory' in smooth air and 'acceptable for normal operation' in moderate turbulence, though it was noted that speed holding required rather more attention than was needed in the 'half air-brake' approach; these ratings were, of course, coloured by the deteriorated dutch-roll behaviour and by the existence of a longitudinal trim change with power.

It should be noted that all approaches in the H.P.115 have been made in daylight and in conditions of reasonable visibility, moreover the final approach leg usually is relatively short, lasting perhaps 30 to 60 seconds; it follows that the ratings quoted above cannot be applied with confidence to long approaches made under adverse weather conditions.

The aircraft's longitudinal static stability was positive, stick fixed, at all speeds, though only marginally so at the highest C_L's reached (see Fig.6); in the stick free case, the aircraft became unstable at speeds greater than

---

* This leads to touch-down in an attitude near the limit for tail clearance so that approaches at lower speeds cannot be carried to completion.

175 knots approximately and was, at best, neutrally stable at speeds below about 90 knots; the manoeuvre margin was positive, stick fixed and free, throughout the speed range. The longitudinal short period oscillation was found to be very heavily damped - nearly dead-beat - at all speeds within the range tested to date (80-175 knots); the lift due to elevator deflection (z_η) is large, but its effects were generally not evident to the pilot (who is seated close to the centre of rotation). These longitudinal characteristics have not produced any handling problems and the pilots have had little difficulty in flying the aeroplane accurately during the low speed tests or, indeed, in any other phase of the programme - the instability at 'high' speeds makes speed control "a little less pleasant" and manoeuvring "a little touchy" but it does not constitute a handling problem. In general, the longitudinal behaviour has been described as "straightforward" and the handling as "pleasant, with control responses that are crisp and precise, and forces that are pleasantly low".

The fairly pronounced ground-effect forecast by wind-tunnel tests has not been detected by the pilots; this may be due to the brief period spent in the region where the ground-effect changes significantly, during the course of a normal take-off or landing. More detailed ground-effect investigations are to be made in the future.

Before closing this section the authors would like to emphasize that, although the H.P.115 has proved to be a remarkable success and unexpectedly docile from the handling point of view, it would be most unwise to infer from this that a larger aircraft of this type, operated under less favourable conditions, would necessarily be equally satisfactory. The performance of the H.P.115 can give no indication of the difficulties associated primarily with sheer size for example, and the attempt to 'read across' to the larger aircraft should be made only with great caution.

8 CONCLUSIONS

Miscellaneous flight tests incidental to the measurement of lateral stability derivatives have been discussed and their results presented. Where possible, these results have been compared with wind-tunnel data, with generally satisfactory agreement; the C_L - α curve obtained as a by-product of these tests agrees particularly well with the wind-tunnel results.

The rudder derivatives (ℓ_ζ, n_ζ, y_ζ) were deduced from the transient response to rudder pulses; the trends shown by these results are similar to those observed in wind-tunnel tests, but the flight derivatives are significantly larger numerically (by up to 25% in the case of n_ζ).

The aileron derivatives (ℓ_ξ, n_ξ) were obtained from tests in which the aircraft was ballasted asymmetrically; owing to instrumentation deficiencies, the derivative y_ξ could not be obtained from these tests. The flight results for ℓ_ξ agree very well with the wind-tunnel over most of the C_L range, but are about 10% low at the highest speed tested - this may well have been due to aeroelastic distortion of the ailerons. Owing to instrumentation deficiencies, the

results obtained for n_ξ could not be established within close limits; the tunnel-flight comparison shows differences of the order of 25%, though the results from the two sources exhibit broadly similar trends.

Derivatives with respect to sideslip were extracted from the results of steady sideslip tests by a method requiring a knowledge of the control derivatives. This was available from flight and wind-tunnel tests and both sets of information were used. The method yielded results for ℓ_v which are in good agreement with the wind-tunnel; the flight results for n_v based on flight data for the control derivatives are in excellent agreement with the wind-tunnel - somewhat fortuitously in view of the uncertainties regarding n_ξ - but the agreement is not good for the results based on wind-tunnel values of the control derivatives; the flight results for y_v agree fairly well with the wind-tunnel data.

A large number of dutch-rolls were recorded under various conditions of flight, and the results have been presented in terms of period, damping and roll/yaw ratio; the oscillation was, at best, lightly damped, and it became divergent at speeds below 70-75 knots. The dutch-roll records were analysed by the time-vector method to yield the lateral stability derivatives ℓ_v, ℓ_p, n_v, n_r, y_v and y_p. The derivatives ℓ_v and n_v obtained by this means agree well with the steady sideslip results, although the wind-tunnel tests would predict a difference of n_v on account of the different sideslip ranges used. The agreement between the two sources is poor in the case of y_v - this is thought to be due to the difficulty of measuring accurately, with the equipment available, the very small lateral accelerations involved. The results obtained for the rotary derivatives ℓ_p, n_r and y_p are somewhat scattered, reflecting the difficulties of measuring phase relationships with sufficient precision; the measured value of ℓ_p agrees reasonably well with theoretical estimates, and y_p shows a similar trend to the estimate, though it differs considerably therefrom. Alternative methods of measuring n_r are being investigated.

The opinions expressed regarding the aircraft's handling qualities have been generally remarkably favourable; in particular the dutch-roll characteristics which, by existing criteria, would have been expected to attract markedly adverse comment, are regarded as at least 'acceptable' at all but the lowest flight speeds achieved. Numerous successful approaches and landings have been made in cross-winds and turbulence levels, relatively high for an aircraft of this low wing-loading.

9 ACKNOWLEDGEMENTS

The authors wish to acknowledge the assistance of their colleagues Mr. J.H. Blackmore and Mr. P.J. Haynes in the work forming the basis of this paper.

The authors also wish to acknowledge the kind co-operation of the Department of Flight, College of Aeronautics, Cranfield, who made available their calibrated 'Dove' aircraft for position-error measurements by the 'formation' method.

SYMBOLS

General

a_y	lateral acceleration at aircraft centre of gravity	(ft/sec^2)
a_{y_i}	lateral acceleration indicated by an accelerometer not at the c.g.	
b = 2s	wing span	(ft)
c	chord	(ft)
c_o	wing centre-line chord	(ft)
g	acceleration due to gravity	32.2 ft/sec^2
L	rolling moment	(lb-ft)
L_1	lift	(lb)
M	pitching moment	(lb-ft)
m	aircraft mass	(slugs)
N	yawing moment	(lb-ft)
OXYZ	system of stability axes	
$OX_BY_BZ_B$	system of body (datum) axes	
$OX_0Y_0Z_0$	system of principal inertia axes	
P	period of oscillation	(sec)
p	rolling velocity	About stability axes. Suffices B or 0 denote velocities about datum or principal inertia axes respectively.
q	pitching velocity	
r	yawing velocity	

SYMBOLS (Continued)

S		wing area	(ft^2)
s		semi-span	(ft)
$T_{\frac{1}{2}}$		time taken for oscillation to decay to one-half its original amplitude	(sec)
u		incremental velocity along OX	
v		incremental velocity along OY	
w		incremental velocity along OZ	
V		true airspeed	(ft/sec) (or knots)
V_i		equivalent airspeed	
W		aircraft weight	(lb)
Y		side force	(lb)
α		wing incidence (= body datum incidence)	(deg)
α_o	$= \alpha + \varepsilon$	incidence of principal inertia axis OX_o	(deg)
β	$= \frac{v}{V}$	angle of sideslip	
γ		inclination of flight path to horizontal	
δ_1		logarithmic increment of dutch-roll oscillation	
ε		inclination of OX_o to OX_B (approximately -3.95°)	
ζ		rudder angle	
ζ_o		rudder angle to trim at zero indicated sideslip	
ζ_d		damping ratio of dutch-roll	
η	$= \frac{\eta_s + \eta_p}{2}$	'elevator' angle	
η_p		port elevon angle	
η_s		starboard elevon angle	

SYMBOLS (Continued)

$\xi = \frac{\eta_s - \eta_p}{2}$ 'aileron' angle

ξ_o aileron angle to trim at zero indicated sideslip

ρ air density

ρ_o air density at 15°C, 1013.2 mb

$\sigma = \frac{\rho}{\rho_o}$ relative density

ϕ bank angle

ψ angle of yaw

A dot above any quantity denotes differentiation with respect to time

A bar above any quantity denotes a time vector

Aerodynamic coefficients and stability derivatives

$C_L = \frac{L_1}{\frac{1}{2}\rho V^2 S}$ lift coefficient

C_{La} 'apparent' lift coefficient $\left(= \frac{W \cos \gamma}{\frac{1}{2}\rho V^2 S} \text{ in unaccelerated flight}\right)$

$\ell_v = \frac{L_v}{\rho V Ss} = \frac{L_\beta}{\rho V^2 Ss}$ derivative of rolling moment due to sideslip,

where $L_v = \frac{\partial L}{\partial v}$, etc

$\ell_p = \frac{L_p}{\rho V Ss^2}$ derivative of rolling moment due to rolling velocity

$\ell_r = \frac{L_r}{\rho V Ss^2}$ derivative of rolling moment due to yawing velocity

$\ell_\zeta = \frac{L_\zeta}{\rho V^2 Ss}$ derivative of rolling moment due to rudder

$\ell_\xi = \dfrac{L_\xi}{\rho V^2 Ss}$ derivative of rolling moment due to aileron

$n_v = \dfrac{N_v}{\rho V Ss} = \dfrac{N_\beta}{\rho V^2 Ss}$ derivative of yawing moment due to sideslip

$n_p = \dfrac{N_p}{\rho V Ss^2}$ derivative of yawing moment due to rolling velocity

$n_r = \dfrac{N_r}{\rho V Ss^2}$ derivative of yawing moment due to yawing velocity

$n_\zeta = \dfrac{N_\zeta}{\rho V^2 Ss}$ derivative of yawing moment due to rudder

$n_\xi = \dfrac{N_\xi}{\rho V^2 Ss}$ derivative of yawing moment due to aileron

$y_v = \dfrac{Y_v}{\rho VS} = \dfrac{Y_\beta}{\rho V^2 S}$ derivative of side force due to sideslip

$y_p = \dfrac{Y_p}{\rho V Ss}$ derivative of side force due to rolling velocity

$y_r = \dfrac{Y_r}{\rho V Ss}$ derivative of side force due to yawing velocity

$y_\zeta = \dfrac{Y_\zeta}{\rho V^2 S}$ derivative of side force due to rudder

$y_\xi = \dfrac{Y_\xi}{\rho V^2 S}$ derivative of side force due to aileron

Inertia characteristics

A_o principal rolling moment of inertia (slugs ft^2)

C_o principal yawing moment of inertia (slugs ft^2)

$A = A_o \cos^2 \alpha_o + C_o \sin^2 \alpha_o$ rolling moment of inertia in stability axes

SYMBOLS (Continued)

C = $C_o \cos^2 \alpha_o + A_o \sin^2 \alpha_o$ yawing moment of inertia in stability axes

E = $(A_o - C_o) \sin \alpha_o \cos \alpha_o$ product of inertia in stability axes

---

REFERENCES

No.	Author	Title, etc.
1	Nethaway, J.E.	Low-speed wind-tunnel calibration of a Mk.9A pitot-static head. ARC 17670, CP 244, March 1955.
2	Letko, W., Danforth, E.C.B.	Theoretical investigation at subsonic speeds of the flow ahead of a slender-inclined parabolic-arc body of revolution and correlation with experimental data obtained at low speeds. NACA T.N.3205, July 1954.
3	Adamson, D.	Errors involved in the measurement of sideslip and dynamic head in the neighbourhood of an aircraft body. R.A.E. Tech. Note Aero 1895, ARC 10885, June 1947.
4	Doetsch, K.H.	The time-vector method for stability investigations. R & M 2945, ARC 16275, August 1953.
5	Rose, R.	Flight measurements of the dutch-roll characteristics of a 60 degree delta wing aircraft (Fairey Delta 2) at Mach numbers from 0.4 to 1.5 with stability derivatives extracted by vector analysis. ARC 23046, CP 653, March 1961.
6	McNeill, W.E., Vomaske, R.F.	A flight investigation to determine the oscillatory damping acceptable for an airplane in the landing approach. NASA Memo 12-10-58A (TIL 6387), February 1959.
7	Lean, D., Eaton, R.	The influence of drag characteristics on the choice of landing approach speeds. ARC 19715, CP 433.

TABLE 1

H.P.115. Principal dimensions and inertia characteristics

Wing	
Gross area (S)	432.5 ft^2
Span (b = 2s)	20 ft
Centre-line chord (c_o)	40 ft
Wing section	Symmetrical, biconvex, circular-arc section: t/c = 6%
Leading-edge sweep	74° 42'
Trailing-edge sweep	0°
Dihedral	0°
Elevons	
Spanwise limits	0.125s-1.0s
Chord, aft of hinge line (C_η)	2.66 ft
Aerodynamic balance	0.52 C_η set-back hinge
Range of movement	$+29^\circ$ to -34°
Spring tab, spanwise limits	0.125s-0.57s
Spring tab, chord	5.4 inches
Spring tab, range	$\pm 12^\circ$
Geared/trim tab, spanwise limits	0.57s-0.9s
Geared/trim tab, chord	5.4 inches
Geared/trim tab, trimming range	$+9^\circ$ to -3°
Geared/trim tab, gear ratio	+0.45 (i.e. anti-balance) (additional ratios 0.3, 0.6 provided)
Fin and rudder	
Gross area (fin + rudder, external to fuselage)	31.3 ft^2
Root chord	7.29 ft
Tip chord	3.9 ft
Leading-edge sweep	60°
Rudder area, aft of hinge-line	8 ft^2
Range of movement (measured in a plane parallel to plane of wing)	$\pm 25^\circ$
Range of movement (measured perpendicular to hinge line)	$\pm 36.5^\circ$
Weight and c.g. position	
Normal all-up weight at engine start	5050 lb
Fuel weight	1170 lb
c.g. position at engine start	0.548 c_o aft of L.E. of centre-line chord

TABLE 1 (Continued)

Inertia characteristics

No fuel	Measured	Firm's estimates
Rolling moment of inertia (A_o)	1,350	1,215 slugs ft^2
Pitching moment of inertia (B)	16,180	15,320 slugs ft^2
Yawing moment of inertia (C_o)	17,380	16,400 slugs ft^2
Full fuel		
Rolling moment of inertia	1,520	1,435 slugs ft^2
Pitching moment of inertia	16,185	15,530 slugs ft^2
Yawing moment of inertia	17,670	16,630 slugs ft^2

The above figures are the principal moments of inertia relevant to the c.g. position of 0.548 c_o.

	Measured	Firm's estimate
Inclination of longitudinal principal inertia axis to body datum axis	-3.95°	-5.1°

This angle did not change significantly with fuel state, and the figures quoted are averages of the 'full' and 'empty' values.

TABLE 2

List of instrumentation

Recorder No.1 S.F.I.M. Type A.22

Quantity measured	Transducer	Type	Range	Natural frequency (c.p.s.)	Damping ratio
Normal acceleration	A.C. accelerometer	Aero Flight	0-2g	12	0.7
Incidence	Wind vane/potentiometer	IT 3-1-16	0-25°	0.064 V_1*	0.025*
Attitude	Pendulum inclinometer	S.F.I.M. J.33	±20°	4	0.2
Pitching velocity	Rate gyroscope	Aero Flight	±10°/sec	10.0	0.7
Port elevon angle	Variable inductance pick-off	Aero Flight	0-20°	-	-
Stb'd elevon angle					

Recorder No.2 S.F.I.M. Type A.26

Quantity measured	Transducer	Type	Range	Natural frequency (c.p.s.)	Damping ratio
Lateral acceleration	A.C. accelerometer	Aero Flight	±0.3g	12	0.7
Sideslip	Wind vane/potentiometer	IT 3-1-16	±5°	0.064 V_1*	0.025*
Rolling velocity	Rate gyroscope	Aero Flight	±30°/sec	17	0.7
Rolling acceleration	Damping current	In item above	±90°/sec^2	Equivalent to maximum trace deflection	
Yawing velocity	Rate gyroscope	Aero Flight	±5°/sec	10.0	0.7
Yawing acceleration	Damping current	In item above	±30°/sec^2	Equivalent to maximum trace deflection	
Rudder angle	Elliott Bros. Variable inductance pick-off	W121-2EB(X)	±25°	-	-
Trim tab angle			-3° + 9°	-	-
Port spring-tab angle			±12°	-	-
Stb'd spring-tab angle			±12°	-	-
Altitude	Static head	Mk.9			
Airspeed	Pitot head	Mk.9			
	Venturi static	Aero Flight			

* Theoretical figures, V_1 in ft/sec.

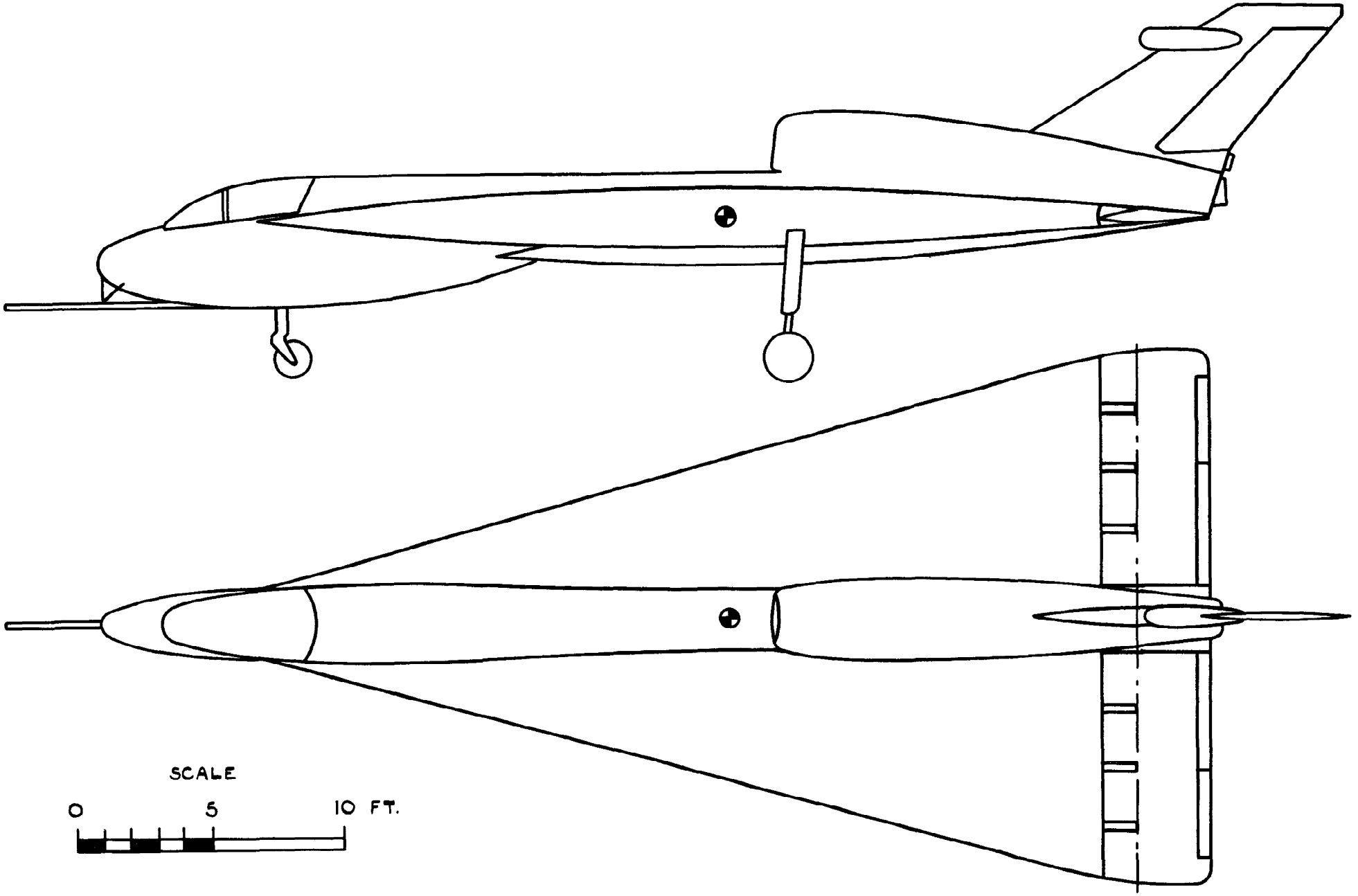

FIG. 1. GENERAL ARRANGEMENT OF HANDLEY-PAGE H.P. 115.

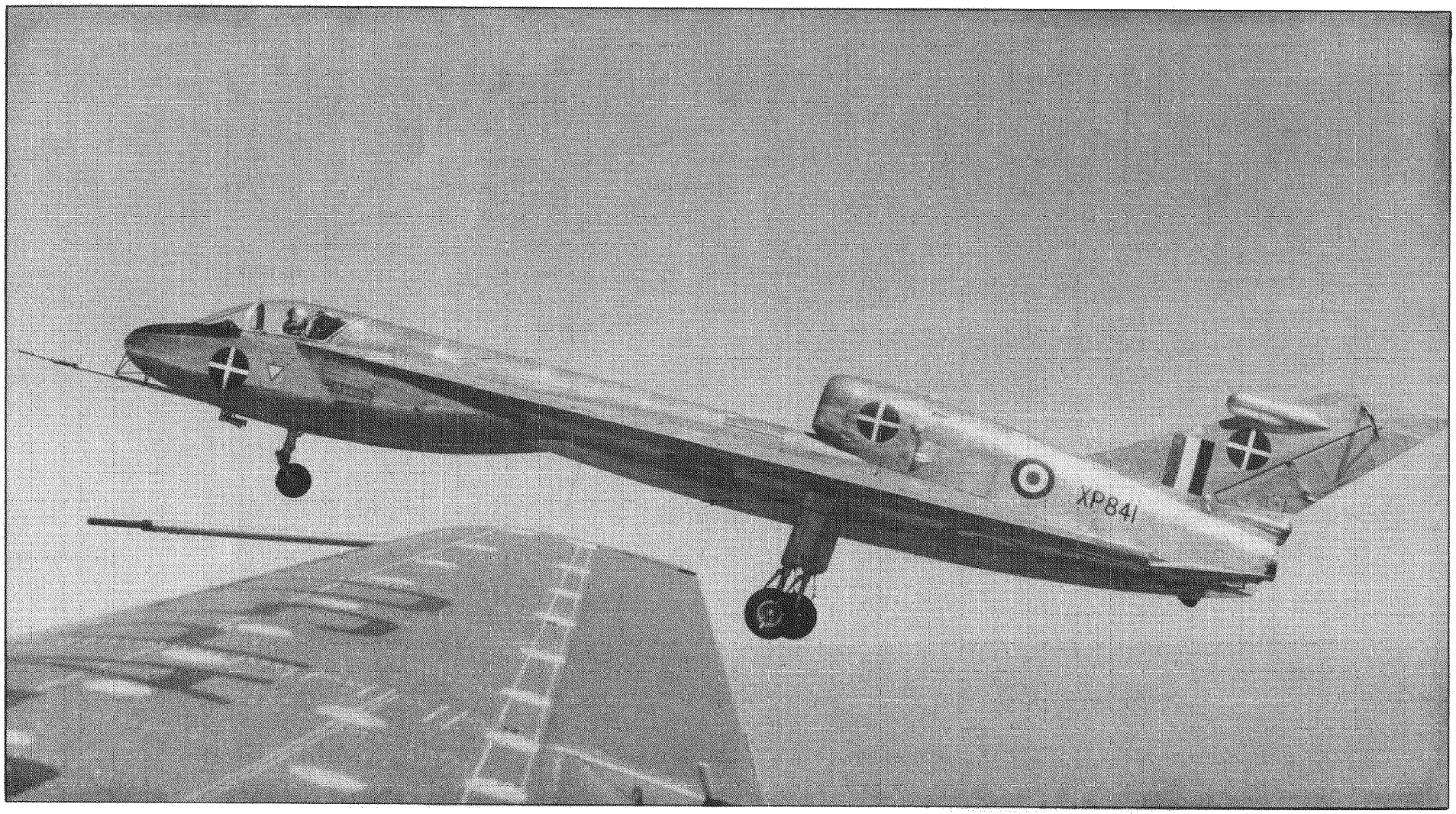

FIG.2. HANDLEY-PAGE H.P.115

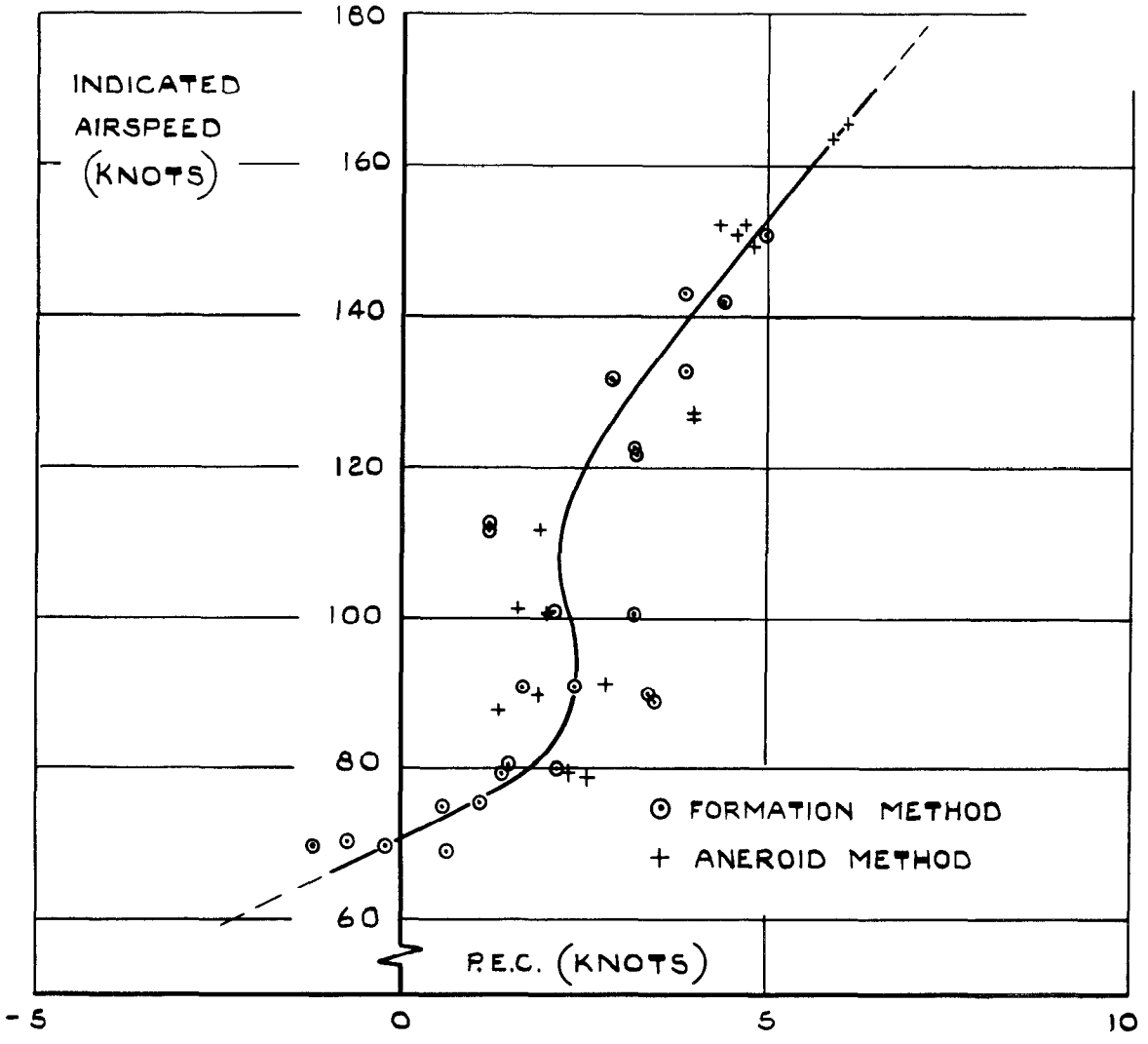

FIG. 3. POSITION ERROR CORRECTION.

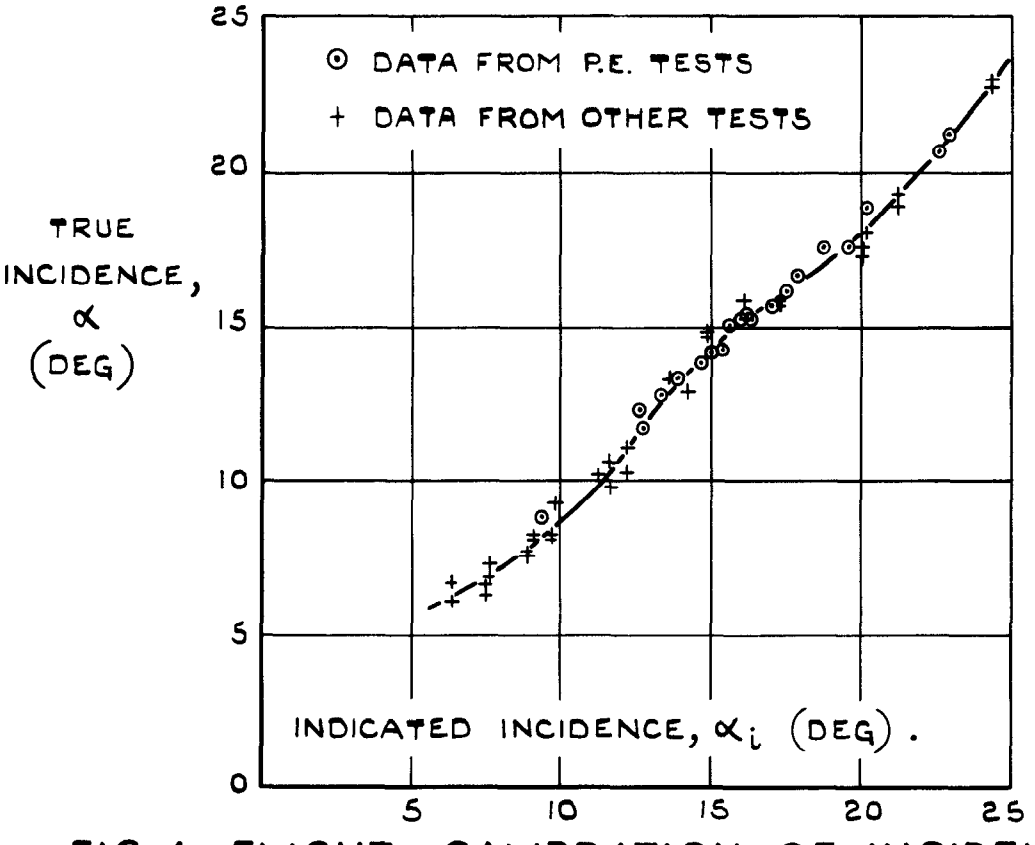

FIG. 4. FLIGHT CALIBRATION OF INCIDENCE VANE.

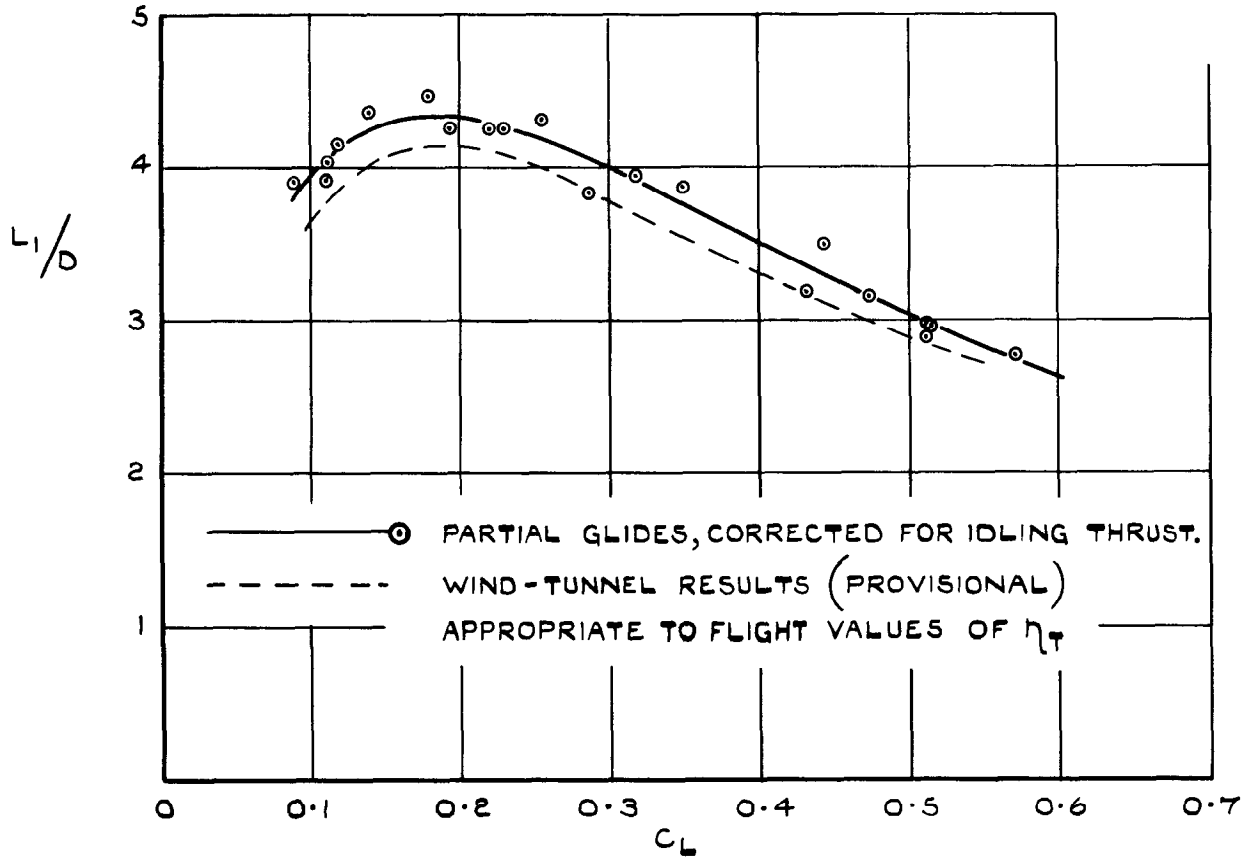

FIG. 5. LIFT – DRAG RATIO.

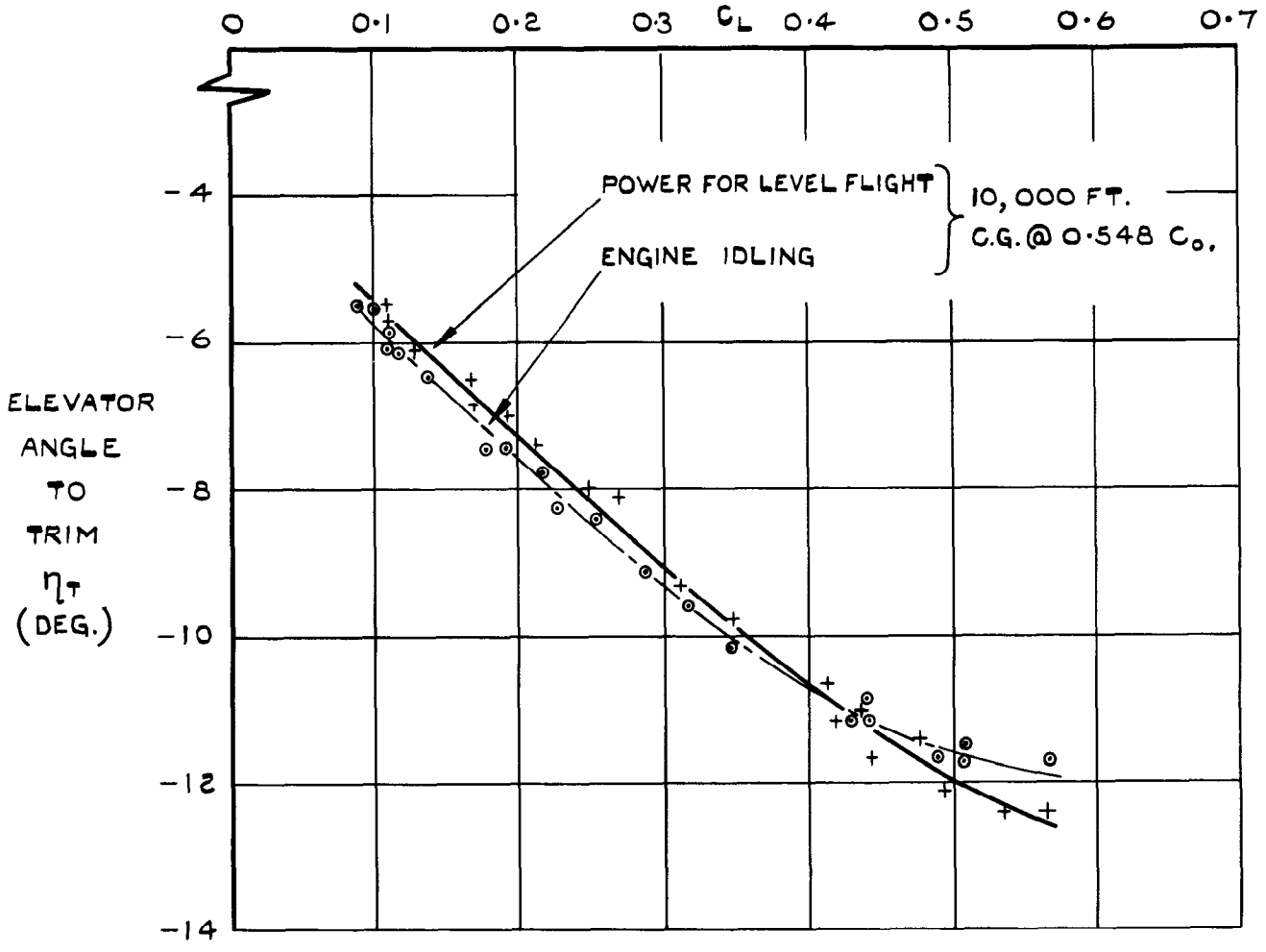

FIG. 6. ELEVATOR ANGLES TO TRIM.

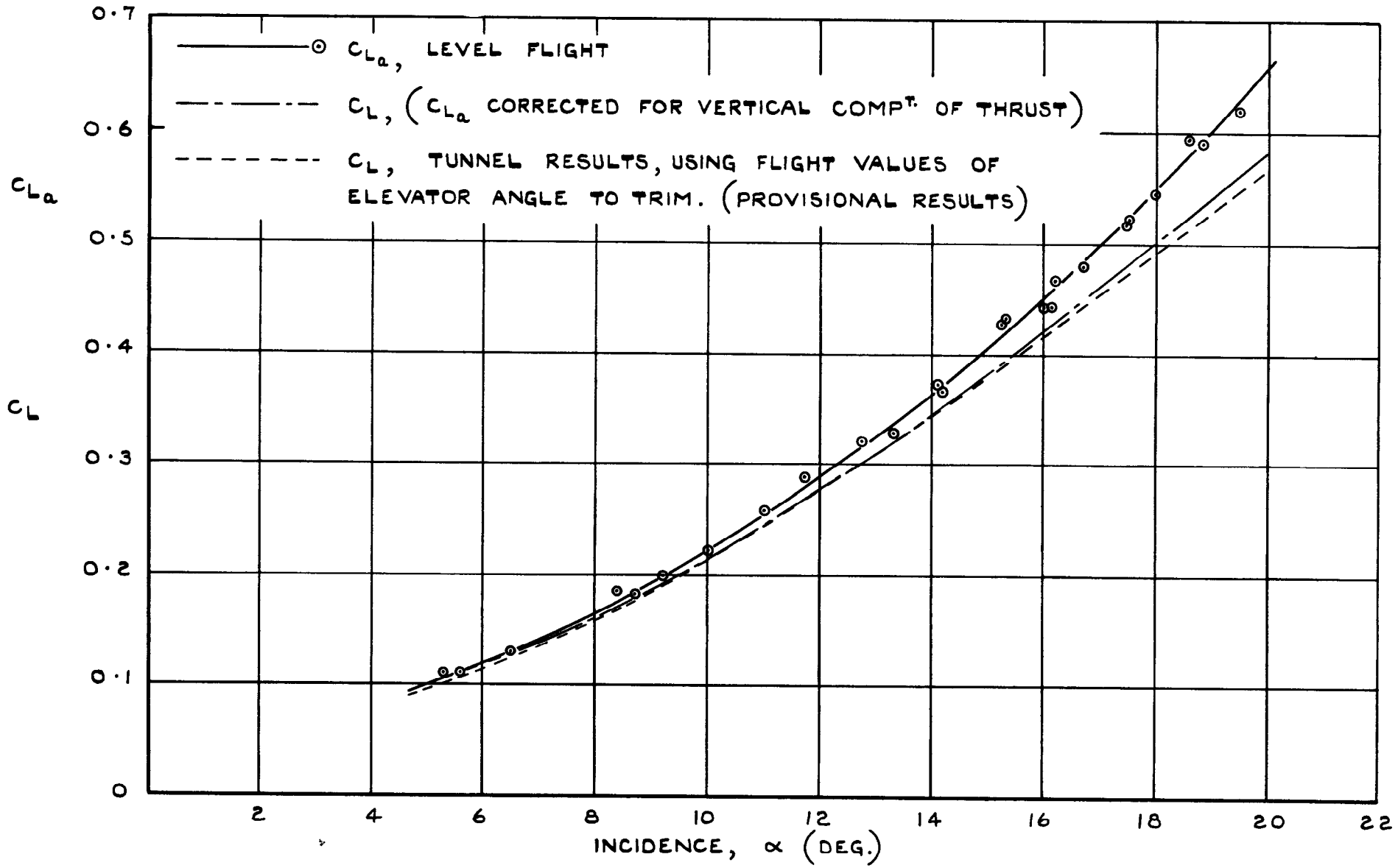

FIG.7. VARIATION OF TRIMMED LIFT WITH INCIDENCE.

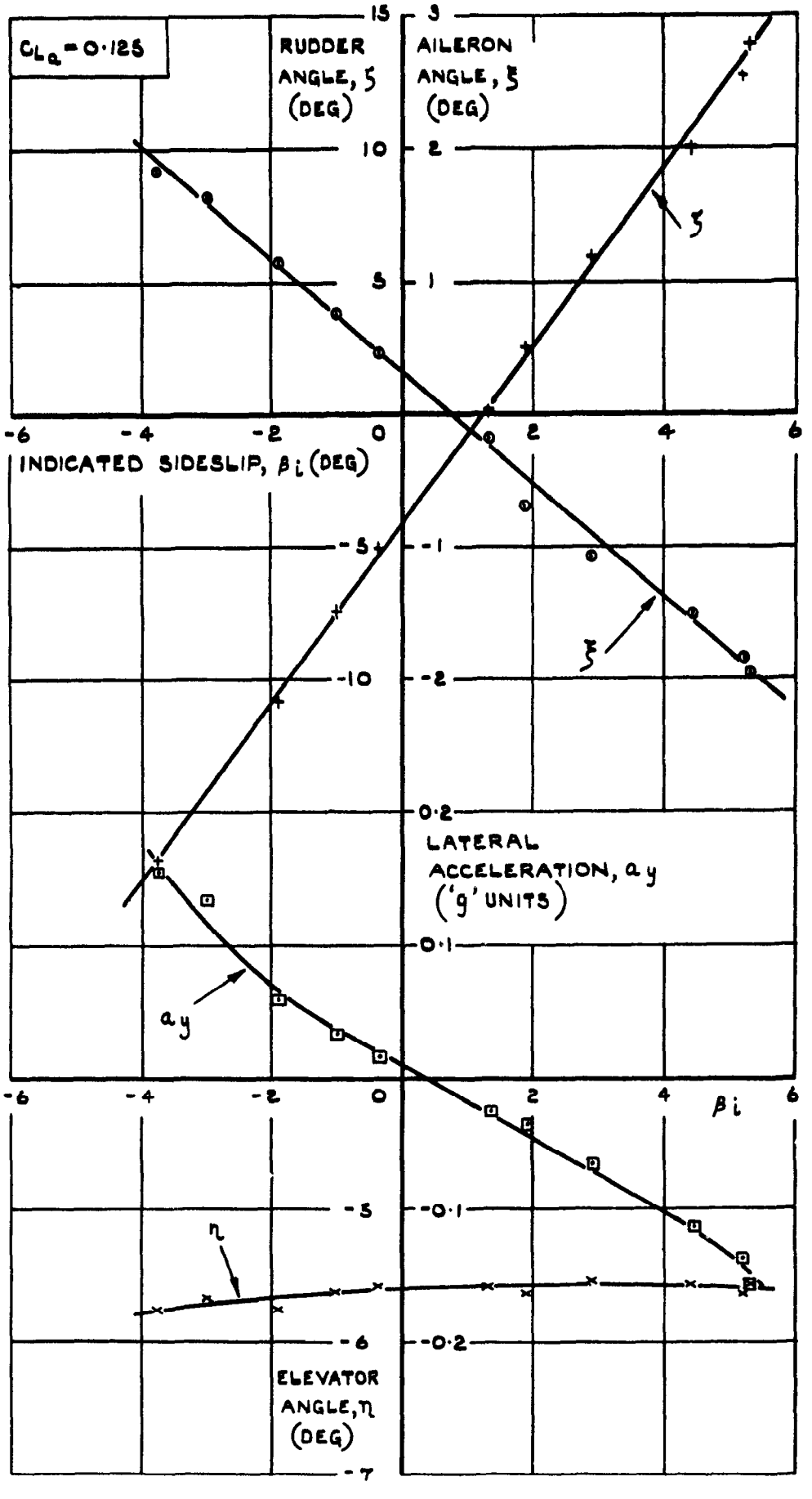

FIG. 8. TYPICAL STEADY SIDESLIP DATA.
(ASYMMETRIC BALLAST – 95LB. PORT.)

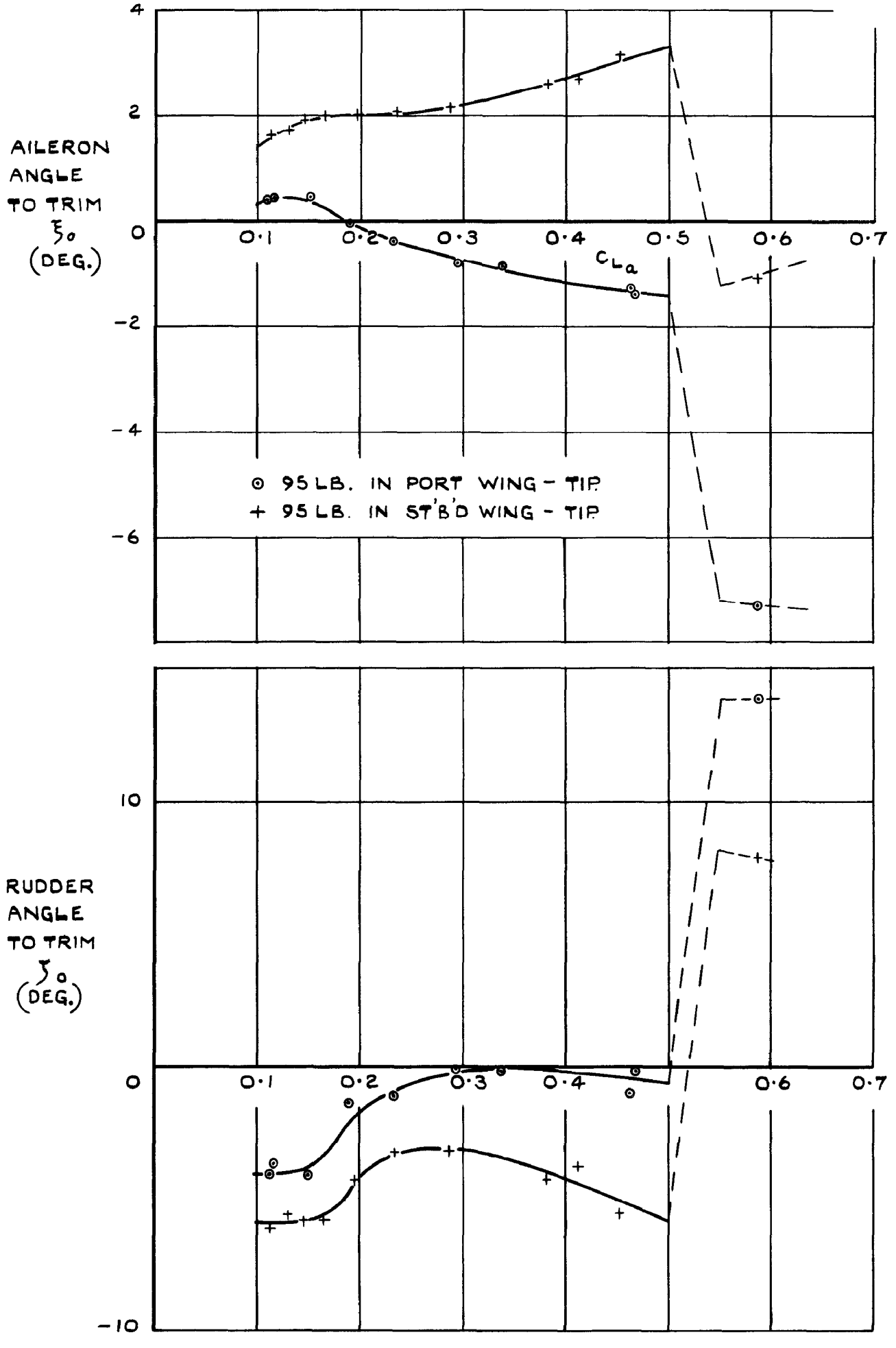

FIG.9. CONTROL ANGLES TO TRIM AT ZERO INDICATED SIDESLIP, WITH ASYMMETRIC BALLAST.

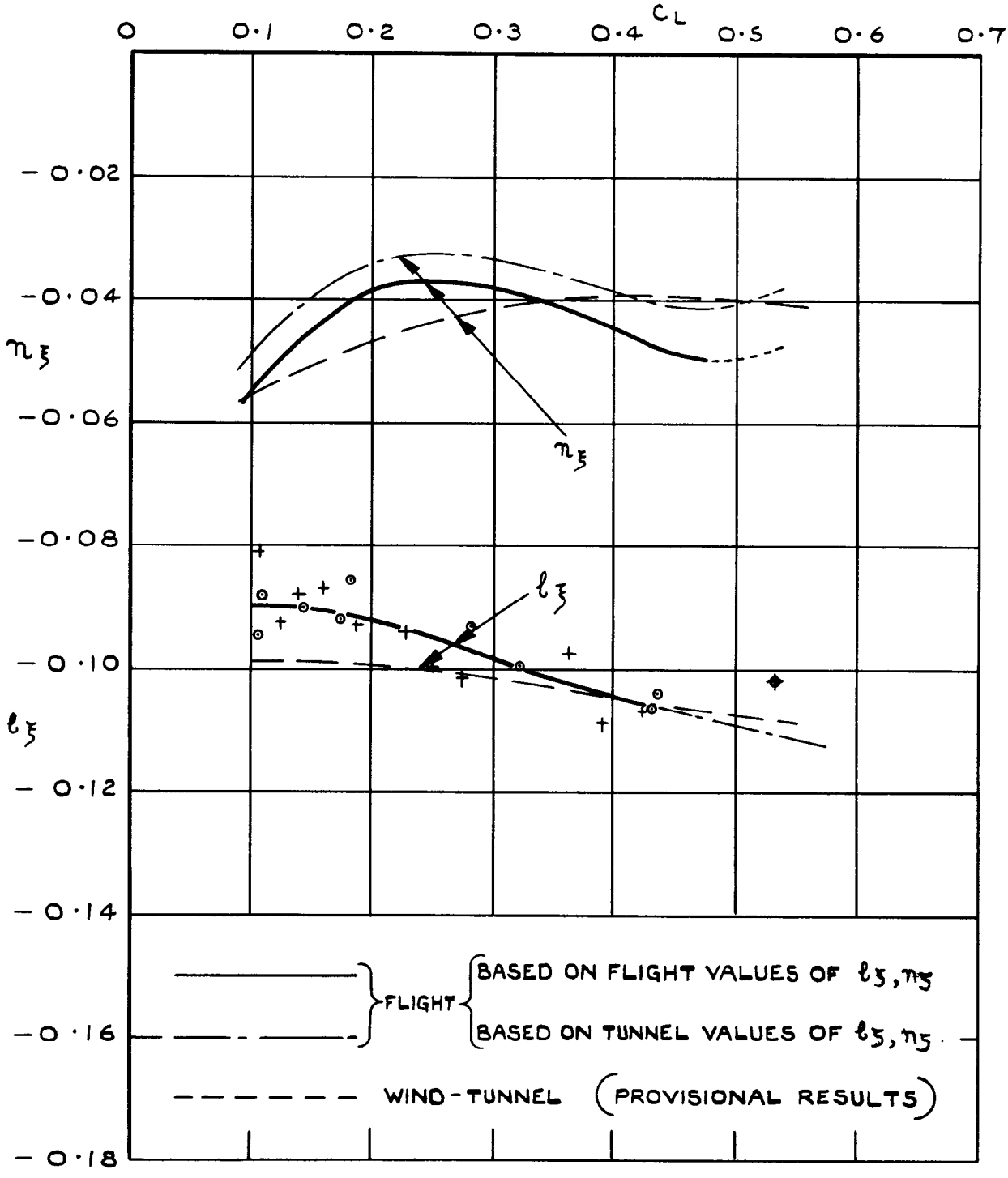

FIG.10. AILERON DERIVATIVES.

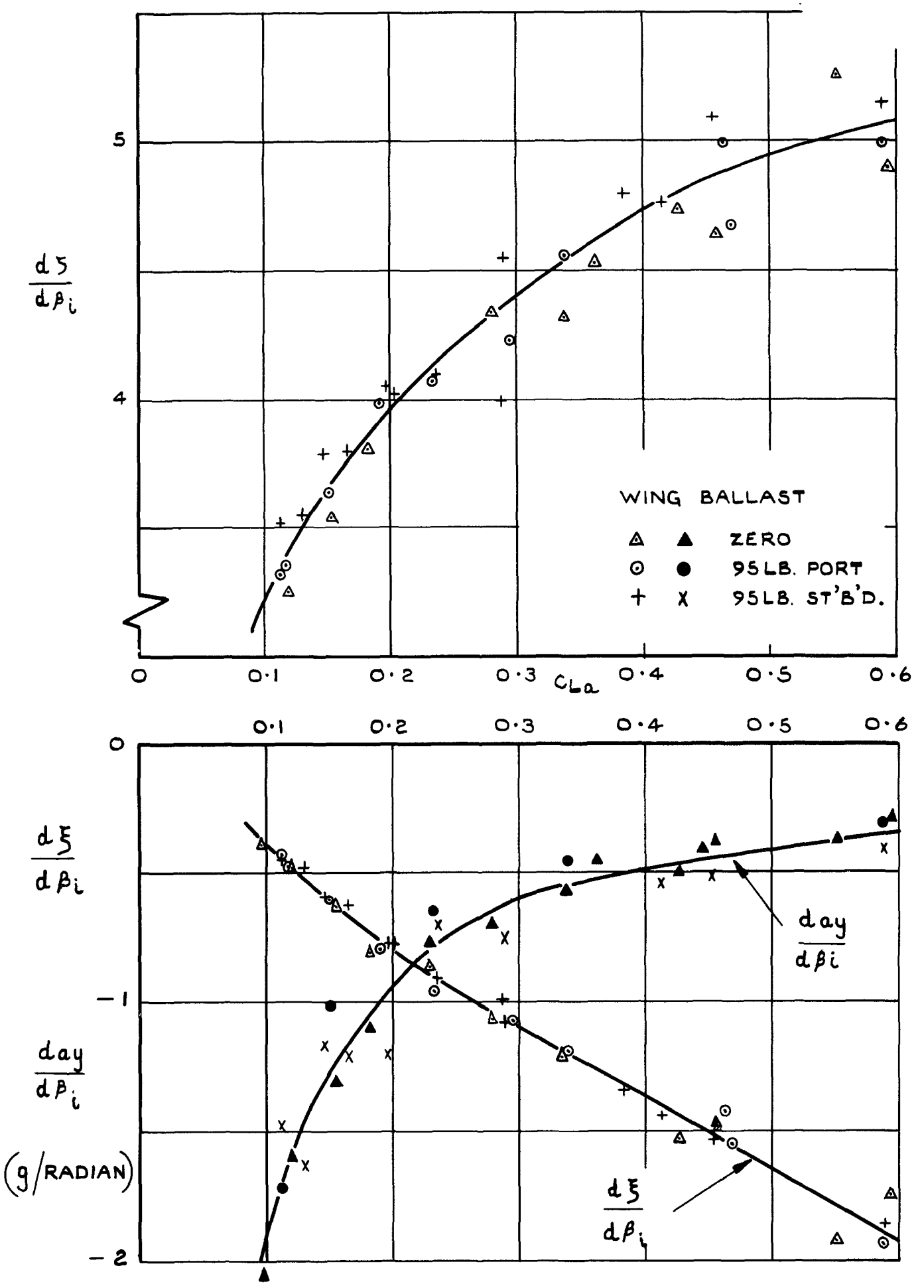

FIG. 11. RATES OF CHANGE OF CONTROL ANGLE AND LATERAL ACCELERATION WITH SIDESLIP.

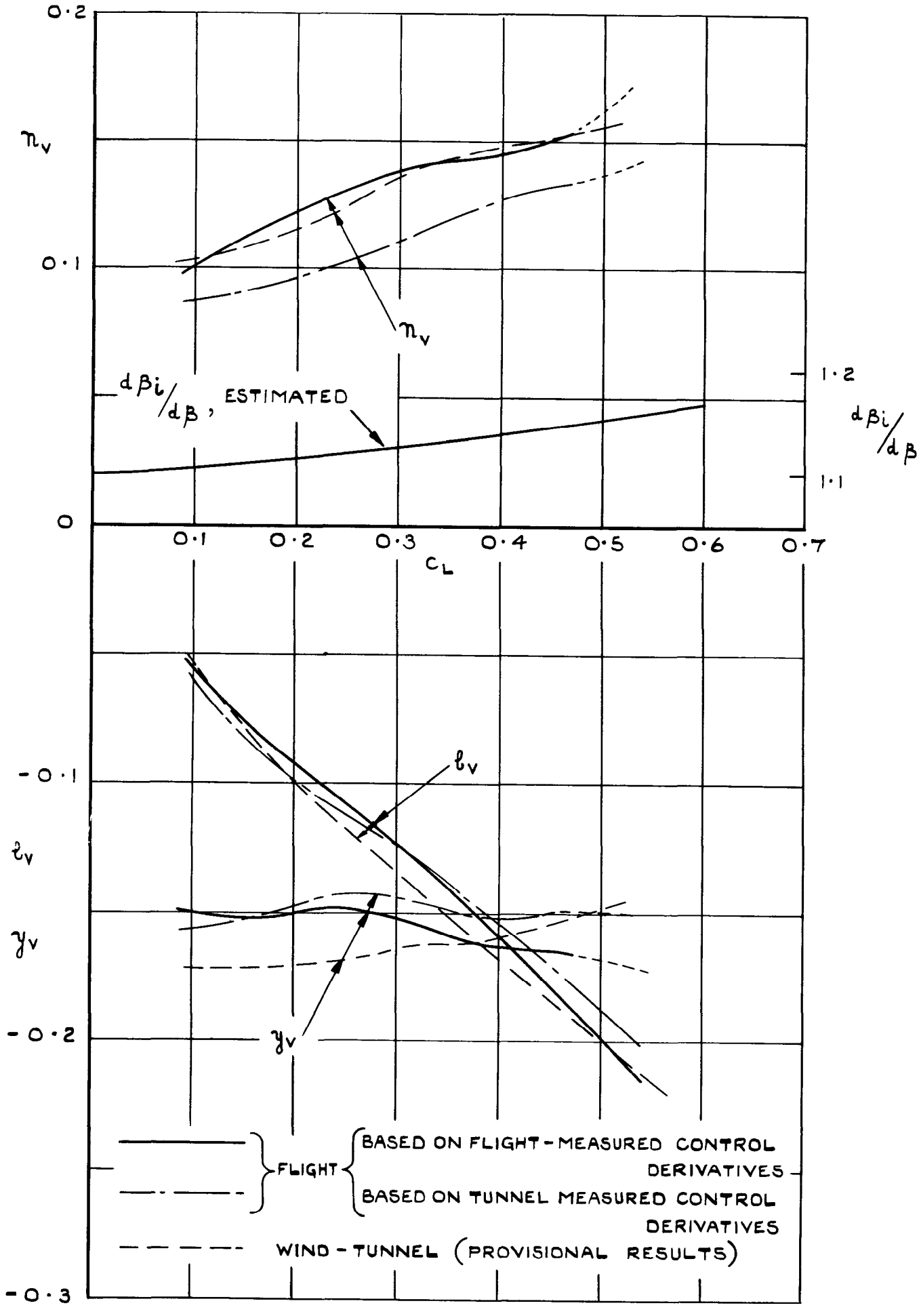

FIG. 12. SIDESLIP DERIVATIVES, FROM STEADY SIDESLIP TESTS.

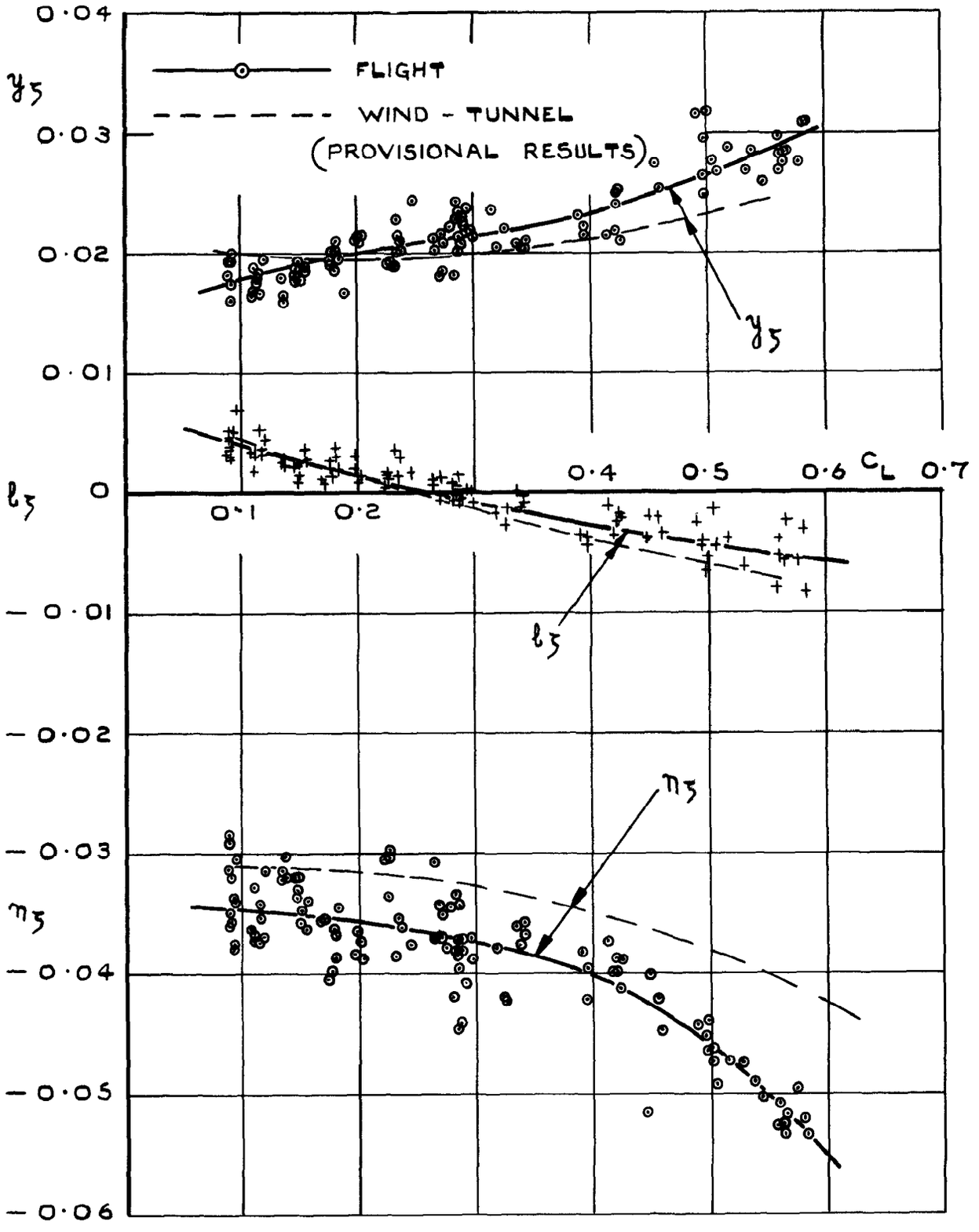

FIG. 13. RUDDER DERIVATIVES.

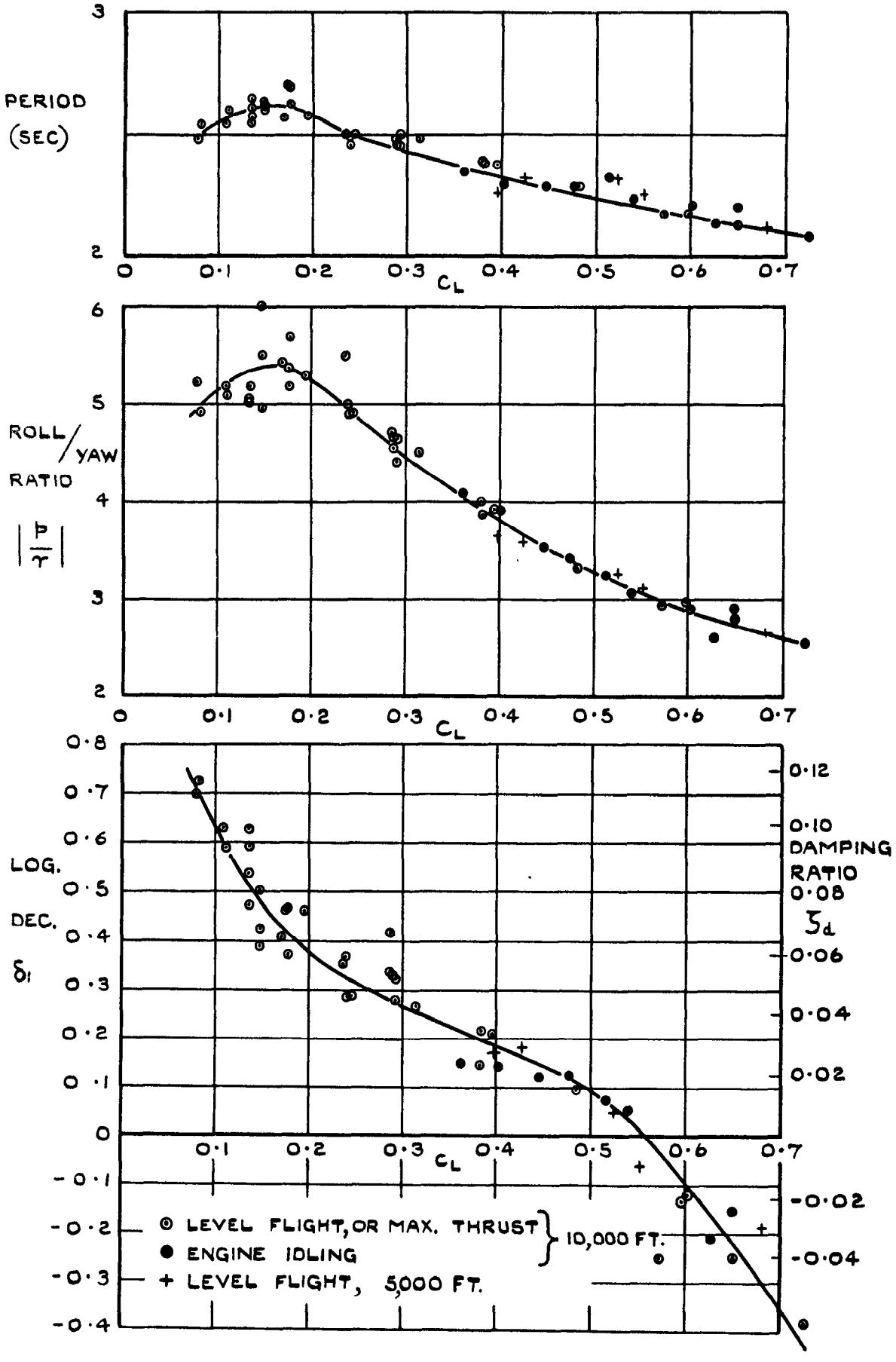

FIG. 14. DUTCH-ROLL CHARACTERISTICS.

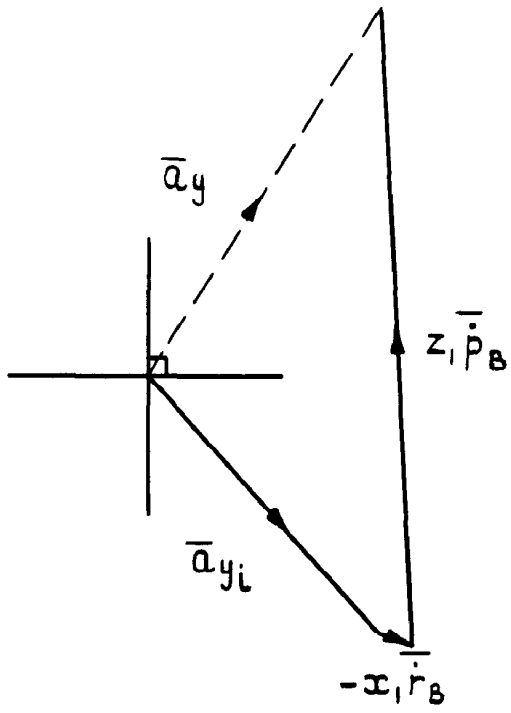

(a) DERIVATION OF LATERAL ACCELERATION AT C.G.

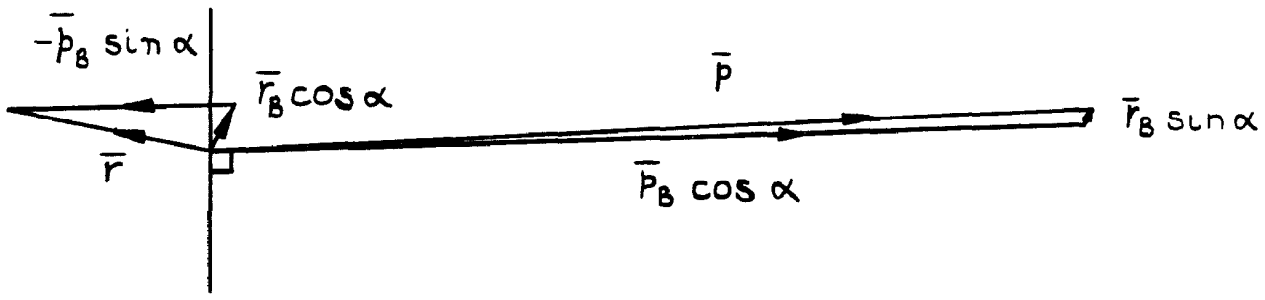

(b) TRANSFORMATION OF ANGULAR RATES FROM BODY TO STABILITY AXES.

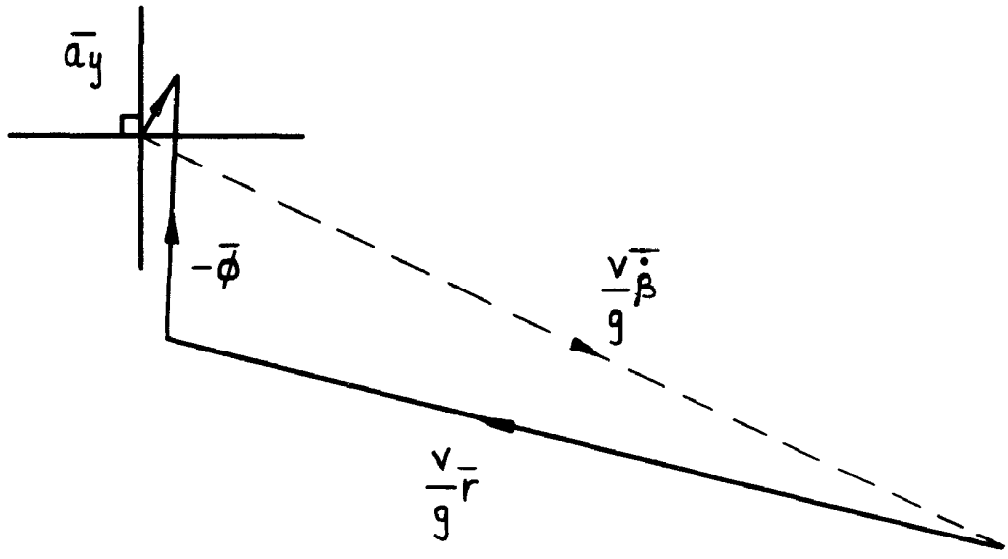

(c) DERIVATION OF SIDESLIP

FIG. 15. PRELIMINARY STAGES IN VECTOR ANALYSIS.

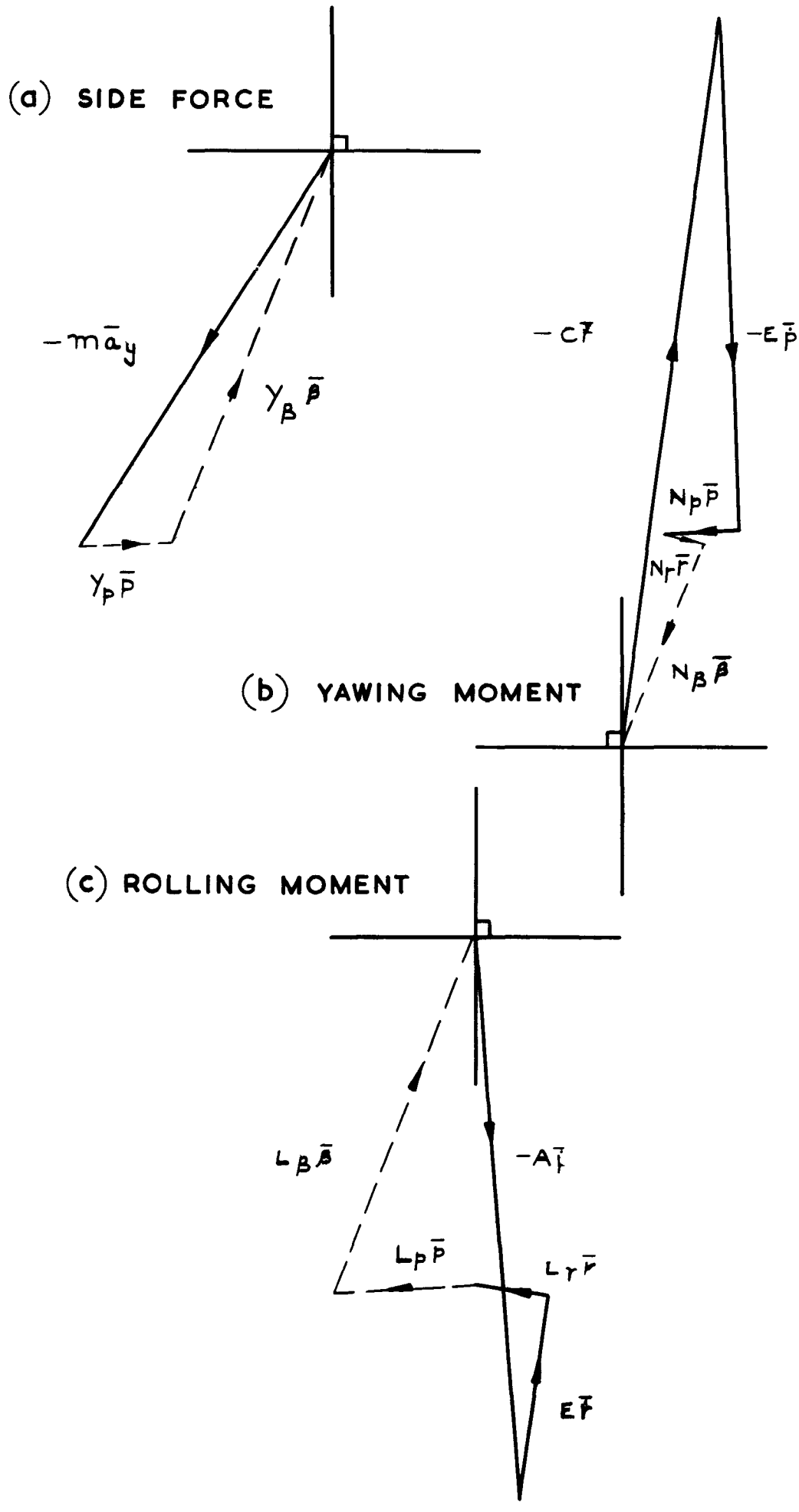

FIG 16. VECTOR POLYGONS OF FORCES AND MOMENTS IN THE DUTCH ROLL.

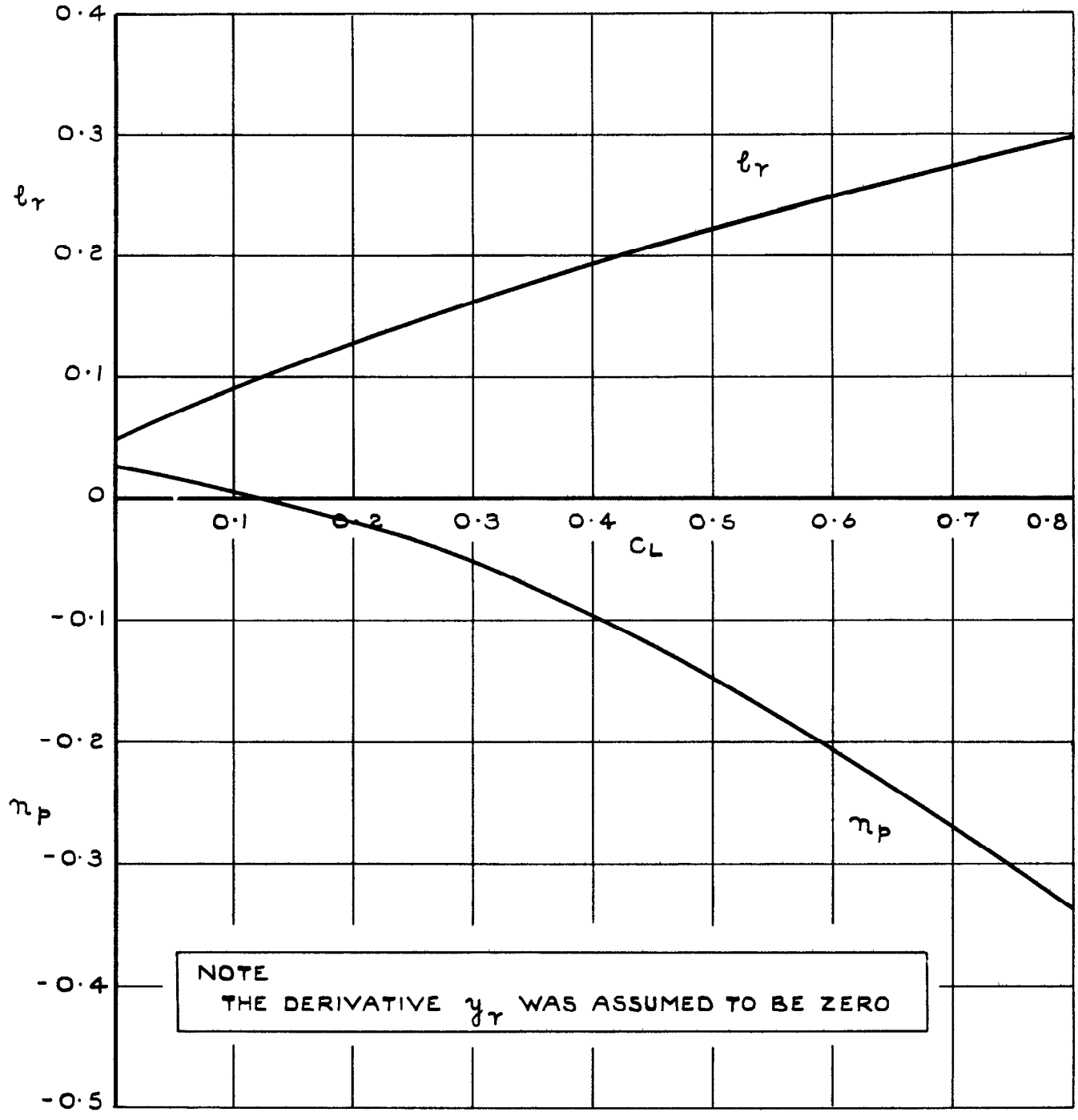

FIG. 17. ESTIMATED DERIVATIVES USED IN VECTOR ANALYSIS.

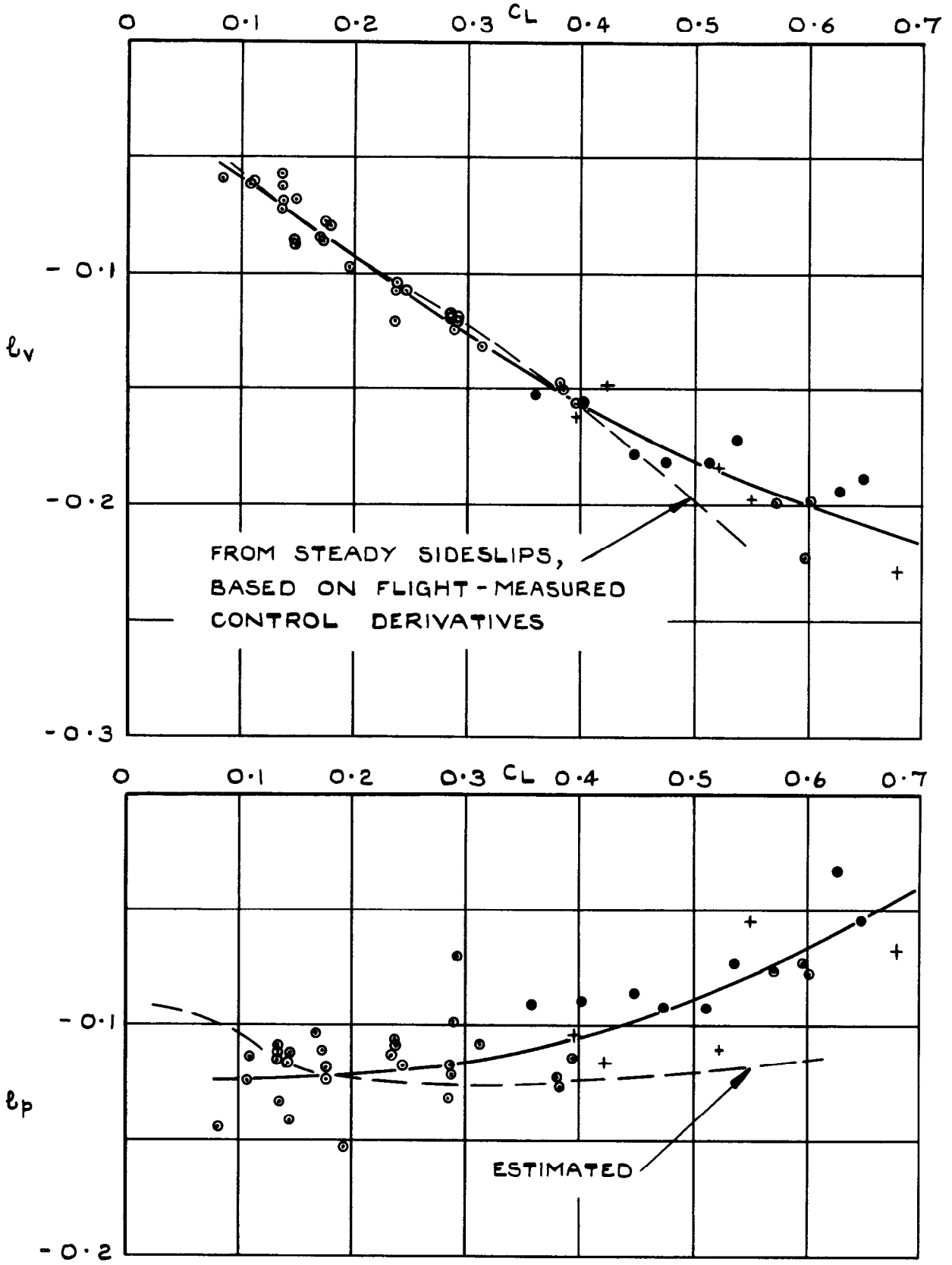

FIG.18. ROLLING MOMENT DERIVATIVES FROM DUTCH - ROLL ANALYSIS.

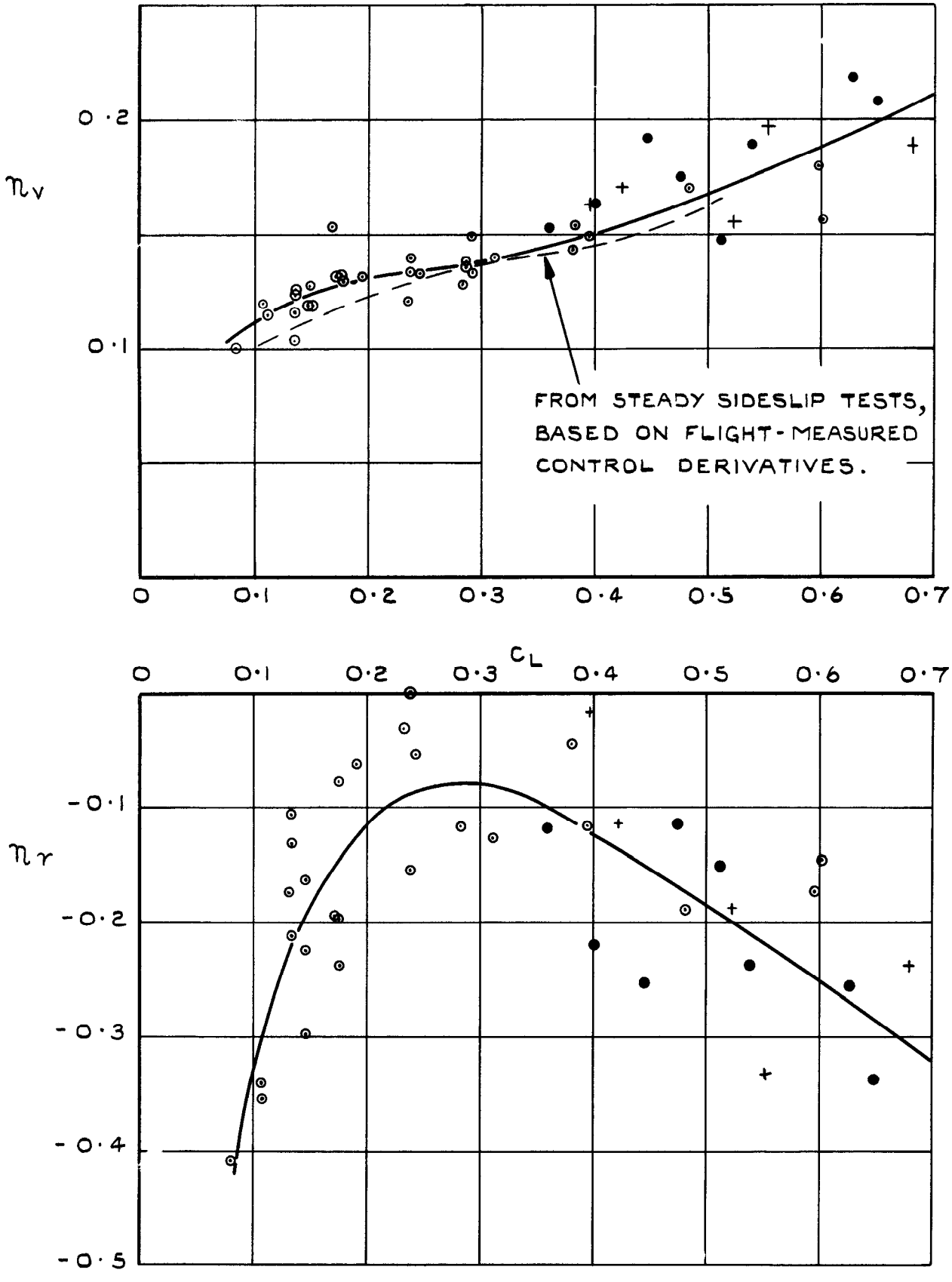

FIG. 19. YAWING MOMENT DERIVATIVES FROM DUTCH-ROLL ANALYSIS.

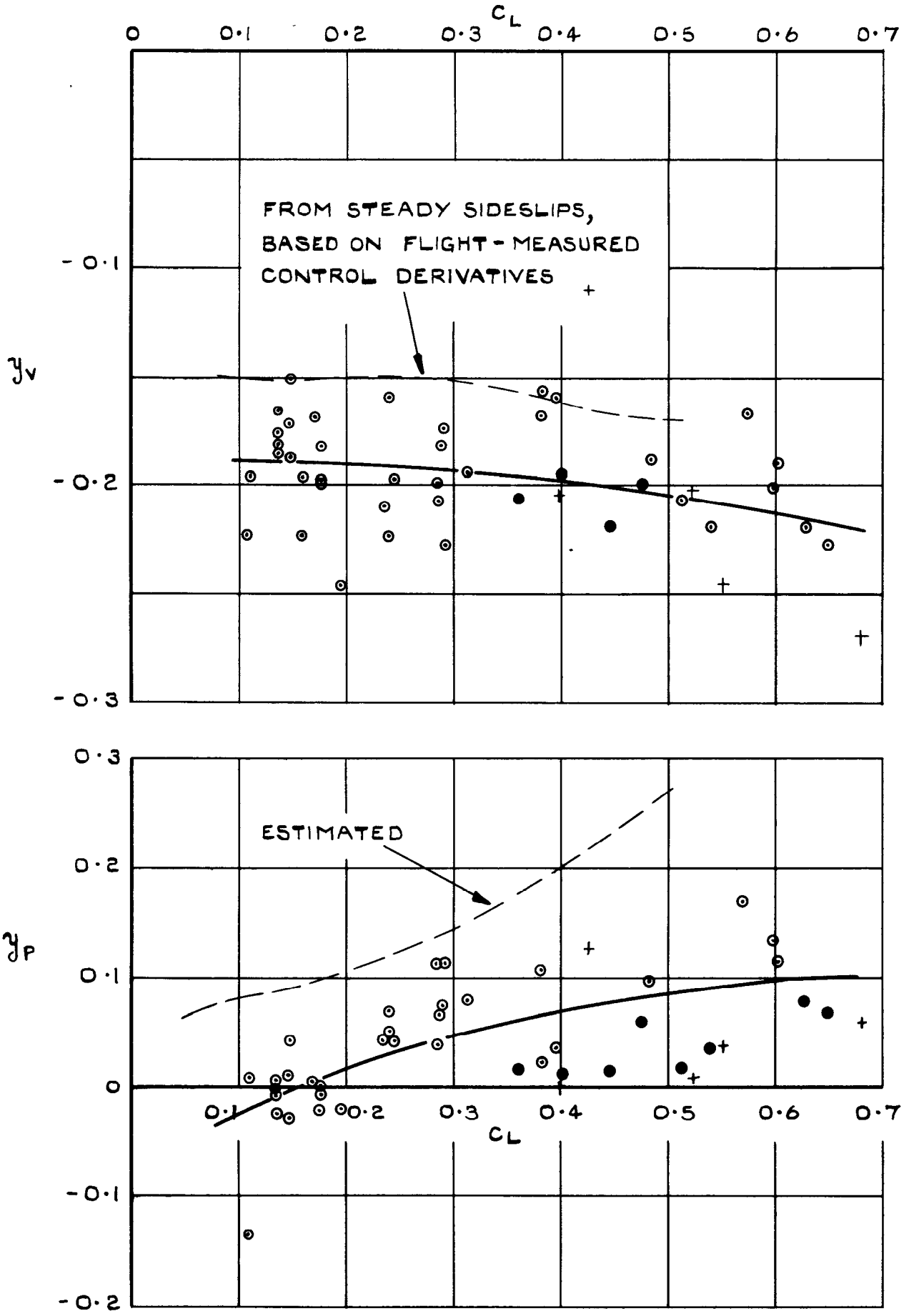

FIG. 20. SIDE-FORCE DERIVATIVES FROM DUTCH-ROLL ANALYSIS.

Printed in England for Her Majesty's Stationery Office by the Royal Aircraft Establishment, Farnborough. Dd.125875. K4.

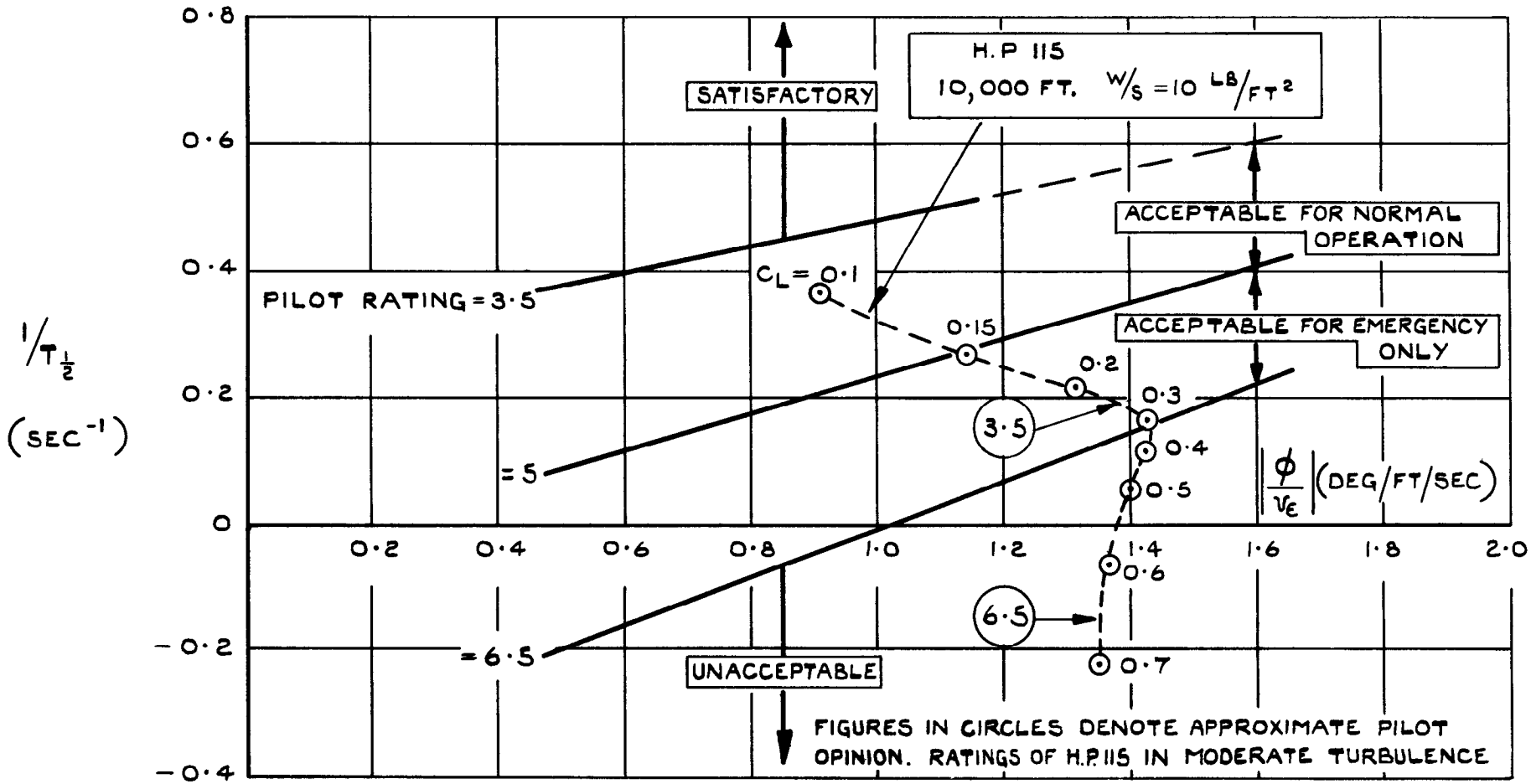

FIG. 21. COMPARISON OF H.P.115 DUTCH ROLL CHARACTERISTICS WITH THE HANDLING CRITERION OF REF. 6.

DETACHABLE ABSTRACT CARDS

Current Paper No. 838

533.6.013.413 :
533.6.013.47 :
533.693.3 :
533.6.011.5

INTERIM REPORT ON LOW-SPEED FLIGHT TESTS OF A SLENDER-WING RESEARCH AIRCRAFT (HANDLEY-PAGE H.P.115).
Bisgood, P.L. and O'Leary, C.O. November 1963.

Tests forming part of a comprehensive programme of lateral stability measurements are described and their results discussed, together with miscellaneous supporting tests. The stability derivatives with respect to aileron deflection (ℓ_ξ, n_ξ) and sideslip (ℓ_v, n_v, y_v) have been measured by static methods, the rudder derivatives (ℓ_ζ, n_ζ, y_ζ) have been deduced from the transient response to rudder pulses, and the derivatives ℓ_v, ℓ_p, n_v, n_r, y_v and y_p have been obtained from time-vector analysis of the dutch-roll mode. Where possible, these results are

(Over)

Current Paper No. 838

533.6.013.413 :
533.6.013.47 :
533.693.3 :
533.6.011.5

INTERIM REPORT ON LOW-SPEED FLIGHT TESTS OF A SLENDER-WING RESEARCH AIRCRAFT (HANDLEY-PAGE H.P.115).
Bisgood, P.L. and O'Leary, C.O. November 1963.

Tests forming part of a comprehensive programme of lateral stability measurements are described and their results discussed, together with miscellaneous supporting tests. The stability derivatives with respect to aileron deflection (ℓ_ξ, n_ξ) and sideslip (ℓ_v, n_v, y_v) have been measured by static methods, the rudder derivatives (ℓ_ζ, n_ζ, y_ζ) have been deduced from the transient response to rudder pulses, and the derivatives ℓ_v, ℓ_p, n_v, n_r, y_v and y_p have been obtained from time-vector analysis of the dutch-roll mode. Where possible, these results are

(Over)

Current Paper No. 838

533.6.013.413 :
533.6.013.47 :
533.693.3 :
533.6.011.5

INTERIM REPORT ON LOW-SPEED FLIGHT TESTS OF A SLENDER-WING RESEARCH AIRCRAFT (HANDLEY-PAGE H.P.115).
Bisgood, P.L. and O'Leary, C.O. November 1963.

Tests forming part of a comprehensive programme of lateral stability measurements are described and their results discussed, together with miscellaneous supporting tests. The stability derivatives with respect to aileron deflection (ℓ_ξ, n_ξ) and sideslip (ℓ_v, n_v, y_v) have been measured by static methods, the rudder derivatives (ℓ_ζ, n_ζ, y_ζ) have been deduced from the transient response to rudder pulses, and the derivatives ℓ_v, ℓ_p, n_v, n_r, y_v and y_p have been obtained from time-vector analysis of the dutch-roll mode. Where possible, these results are

(Over)

Current Paper No. 838

533.6.013.413 :
533.6.013.47 :
533.693.3 :
533.6.011.5

INTERIM REPORT ON LOW-SPEED FLIGHT TESTS OF A SLENDER-WING RESEARCH AIRCRAFT (HANDLEY-PAGE H.P.115).
Bisgood, P.L. and O'Leary, C.O. November 1963.

Tests forming part of a comprehensive programme of lateral stability measurements are described and their results discussed, together with miscellaneous supporting tests. The stability derivatives with respect to aileron deflection (ℓ_ξ, n_ξ) and sideslip (ℓ_v, n_v, y_v) have been measured by static methods, the rudder derivatives (ℓ_ζ, n_ζ, y_ζ) have been deduced from the transient response to rudder pulses, and the derivatives ℓ_v, ℓ_p, n_v, n_r, y_v and y_p have been obtained from time-vector analysis of the dutch-roll mode. Where possible, these results are

(Over)

compared with wind-tunnel tests; the agreement is satisfactory in the case of the aileron and sideslip derivatives measured under static conditions, and ℓ_v and n_v obtained from dutch-roll analysis agree well with the 'static' results.

A brief report on the more important handling qualities is included. Contrary to expectation, the handling of the aircraft is free from serious problems.

compared with wind-tunnel tests; the agreement is satisfactory in the case of the aileron and sideslip derivatives measured under static conditions, and ℓ_v and n_v obtained from dutch-roll analysis agree well with the 'static' results.

A brief report on the more important handling qualities is included. Contrary to expectation, the handling of the aircraft is free from serious problems.

compared with wind-tunnel tests; the agreement is satisfactory in the case of the aileron and sideslip derivatives measured under static conditions, and ℓ_v and n_v obtained from dutch-roll analysis agree well with the 'static' results.

A brief report on the more important handling qualities is included. Contrary to expectation, the handling of the aircraft is free from serious problems.

compared with wind-tunnel tests; the agreement is satisfactory in the case of the aileron and sideslip derivatives measured under static conditions, and ℓ_v and n_v obtained from dutch-roll analysis agree well with the 'static' results.

A brief report on the more important handling qualities is included. Contrary to expectation, the handling of the aircraft is free from serious problems.

Published by
HER MAJESTY'S STATIONERY OFFICE

To be purchased from
49 High Holborn, London W.C.1
423 Oxford Street, London W.1
13A Castle Street, Edinburgh 2
109 St. Mary Street, Cardiff
Brazennose Street, Manchester 2
50 Fairfax Street, Bristol 1
35 Smallbrook, Ringway, Birmingham 5
80 Chichester Street, Belfast 1
or through any bookseller

C.P. No. 838

S.O. CODE No. 23-9016-38